Stefan MARKO

Surface Electromyography-based Detection of Human Hand Motions

Diploma Thesis

TU Graz

Technische Universität Graz

Istitut für Semantische Datenanalyse

Graz University of Technology

Krenngasse 37; 8010 Graz

Head: Assoc.Prof. Dipl.-Ing. Dr.techn. Gernot Müller-Putz

Supervisor

Dipl.-Ing. Dr.techn. Reinhold Scherer

Evaluator

Dipl.-Ing. Dr.techn. Reinhold Scherer

Graz, May 2012

EIDESSTATTLICHE ERKLÄRUNG

Ich erkläre an Eides statt, dass ich die vorliegende Arbeit selbstständig verfasst, andere als die angegebenen Quellen/Hilfsmittel nicht benutzt, und die den benutzten Quellen wörtlich und inhaltlich entnommenen Stellen als solche kenntlich gemacht habe.

Graz, am ....
                                                        (Unterschrift)

STATUTORY DECLARATION

I declare that I have authored this thesis independently, that I have not used other than the declared sources / resources, and that I have explicitly marked all material which has been quoted either literally or by content from the used sources.

....
date   (signature)

I

Acknowledgements

First of all, I want to express my gratitude my supervisor, Reinhold Scherer, who always took the time to answer my questions and helped me whenever problems showed up.

I also want to thank all the people at the Laboratory of Brain-Computer Interfaces who always provided good input and offered their help.

Many thanks also go to my family who supported me throughout all the years both mentally and financially.

Finally, i also want to thank my girlfriend Karin for her understanding and patience during my studies.

Abstract

The surface electromyogram (sEMG) of the human forearm provides useful information about the activation of different muscles during the exertion of movements and can be used as a reliable control signal for active prostheses. In this diploma thesis an online classification system to distinguish between ten different hand and wrist movements with a low latency has been implemented and tested. The classification system for this thesis is based on an onset detection algorithm and a Support Vector Machine Classifier.

As a first step, the performance of different sEMG feature extraction methods in the time and frequency domain were compared with regards to their cross validation performance. Additionally, the online system has been tested on ten subjects in a cue-based scenario using the best performing single feature for each subject. For seven of the ten subjects the Willison amplitude feature showed the best performance. The system showed an overall performance of 92.75% across all subjects in the ten-class problem and the latency was below 300 ms.

The developed system was then used in a self-paced scenario to control the computer game Portal 2 using nothing but the sEMG signals as control inputs. Two users successfully used this system to play two levels of the game. The level completion time has been compared between the implemented sEMG game control system and the mouse as a conventional input modality. The level completion times for the sEMG-based system were about four times as high as those for the mouse-controlled scenario.

In addition to this, a seven class EMG classification system has been combined with a Steady-State Visual Evoked Potential (SSVEP) BCI to form a hybrid Brain-Computer Interface (hBCI) and the resulting system has again been used to control Portal 2. Two users completed the same two levels as before using this system. The level completion times with this system are in the same range as in the EMG game control scenario.

Keywords: Surface Electromyography, Active Prostheses, Support Vector Machine, Pattern Recognition, Transradial Amputee

Kurzfassung

Das Oberflächen-Elektromyogramm (sEMG) des menschlichen Unterarmes liefert wertvolle Informationen über die Aktivierung verschiedener Muskelgruppen während der Ausführung von Bewegungen und kann als zuverlässiges Kontrollsignal für aktive Prothesen benutzt werden. In dieser Arbeit wurde ein Klassifikationssystem implementiert und getestet, das in der Lage ist mit geringer Latenzzeit zwischen verschiedenen Hand- und Handgelenksbewegungen zu unterscheiden. Das in dieser Arbeit implementierte System basiert auf einem Algorithmus zur Detektion eines Bewegungsanfangs und einer Support Vector Maschine als Klassifikator.

Als ein erster Schritt wurden verschiedene Featureextraktionsmethoden für das sEMG im Zeit- und bezüglich ihrer Kreuzvalidierungsergebnisse miteinander verglichen und das Onlinesystem einem Test mit zehn Probanden unterzogen wobei das jeweils beste Feature für den jeweiligen Probanden benutzt wurde. Für sieben der zehn Probanden wurde die Willison Amplitude als bestes Feature ausgewählt. Das Onlinesystem zeigte eine Gesamtleistung von 92.75% für das Zehn-Klassen-Problem, wobei die Latenzzeit unter 300 ms betrug.

Das System wurde anschließend in einem Experiment zur Steuerung des Computerspiels Portal 2 benutzt. Hierbei wurden keine anderen Eingabegeräte als das vorgestellte System benutzt. Zwei Probanden testeten das System und waren in der Lage, das Spiel erfolgreich zu steuern und zwei verschiedene Levels abzuschließen. Die zur Bewältigung der beiden Levels benötigten Zeiten wurden dabei mit den Zeiten verglichen die benötigt wurden, wenn das Spiel mit der Maus gesteuert wurde. Die mit dem implementierten System benötigten Zeiten waren hierbei in etwa viermal so lang wie jene, die mit der konventionellen Steuerung über die Maus erreicht wurden.

Zusätzlich wurde das Klassifikationssystem mit einem Steady-State Visual Evoked Potential (SSVEP) Brain-Computer Interface (BCI) zu einem hybriden BCI (hBCI) kombiniert und das resultierende Gesamtsystem wiederum zur Bewältigung der beiden Levels in Portal 2 genutzt. Die zur Bewältigung der Level benötigten Zeiten liegen hierbei wiederum im selben Bereich wie im EMG-gesteuerten Fall.

Stichwörter: Oberflächen-Elektromyographie, Aktive Prothesen, Support Vector Maschine, Mustererkennung, Transradiale Amputation

Contents

1 Introduction

The human hand is a highly dexterous tool that has 22 degrees of freedom (DOF) [61]. The importance of this tool in our everyday life is extremely high and many of our daily chores cannot, or at least not in the usual way, be done without using our hands. This immediately becomes very present to anyone who suffers from a fracture in the upper extremity and gets a cast on one, or even worse, both arms. But fractures only represent a temporal handicap since the human body is very good at restoring its functionality. There are however conditions where the capability of the body to heal itself reaches its limitations. Some medical conditions or accidents require a total or partial amputation of the upper extremity. This permanent loss of the hand represents a major limitation and handicap to the amputee. A total restoration of the functionality of the human hand would hence represent a huge gain of life quality to those handicapped persons. This is the reason why a lot of research is conducted in the area of highly dexterous active hand prostheses (AHP). Due to advances in microelectronics and mechanics, it is already possible to construct very complex robotic prostheses that offer (almost) the full functionality of a healthy human hand and a large number of DOF. An overview of AHP that are currently available or under development can be found in [2; 12].

Providing a device that is capable of replacing the functionality of the human hand is only one part of the problem, however. The other issue is to actually control the prosthesis. One of the most intuitive (and very common) ways to derive some sort of control signal for the artificial limb is to use the activation of the remaining muscles that actually controlled the movements of the real hand before the amputation. The signal that can be derived from the activation of the muscle is called the electromyogram (EMG) or, if only noninvasive recording techniques are used, the surface electromyogram (sEMG). Using the sEMG has the advantage of being of very little risk to the subject. Also, no specially trained personnel is needed for the application of the electrodes. In addition, no significant difference was found when the decoding accuracy of the intramuscular EMG was compared to that of the sEMG signals in wrist and grip movements [25]. Many research groups are working on the usage of the sEMG to control upper limb function [8; 13; 20; 34; 38; 44; 45; 52; 61]. However, Zecca et al. in 2002 [61] stated that no control system offers the high level of control required by the complex active prostheses and this still is a problem up to now. Also, the latency of the control system has to be kept low. In fact, the time it takes for the system to respond to a input must be lower than 300 ms in order to reduce the lag perceived by the user [30].

The usage of remaining muscles may not always be possible, especially in the case of total amputation. Otto Bock (Otto Bock Health-Care Products, Austria) have developed a prosthesis that is capable of replacing some of the functionality of a complete lost arm by using the sEMG of the surgically separated and re-innervated pectoralis muscle (Figure 1.1). This process is called targeted muscle re-innervation (TMR).
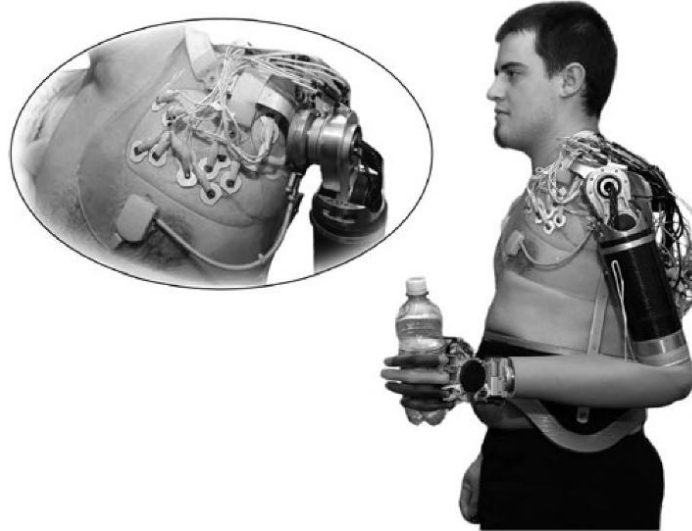
Figure 1.1: A prosthesis presented by Otto Bock (Otto Bock HealthCare Products, Austria). This prosthesis offers seven degrees of freedom and is controlled via signals recorded from the pectoralis muscle. The muscle has been surgically separated and reinnervated in a process called targeted muscle reinnervation (TMR).

However, for transradial amputees, where the amputation is conducted above the wrist, such a complex procedure is not necessary since there are remaining muscles in the forearm. In this case the sEMG of these muscles can be used to control an artificial limb.

But how exactly can these signals be used to control a multifunctional prosthesis? One solution is to relate the muscle activation that once lead to a movement of the real hand to the control signals for the robotic hand. In principle, there are two different ways of doing this. One way is to apply a regression algorithm to make a connection between the muscle activation and an *analogue* control signal for the prosthesis, allowing progressive control of the prosthesis. The second way, that is most commonly found in literature, is to apply classification to map the values of several features that are extracted from the sEMG signals to *integer* values representing different class labels. Since most of the research groups deal with the problem using a classification algorithm, this method will also be used in this thesis as a first approach. The concept of the movement classification

system that will be implemented for this thesis can be found in Figure 1.2. It basically starts with the subject performing a movement and the recording of the corresponding sEMG signal. To keep the latency of the system low, it was decided to use the initial muscle activity after the beginning of a movement for the classification instead of the end positions. To achieve this, some sort of onset detection has to be implemented to find the beginning of a movement and determine the data segment for feature extraction (indicated by the green and red lines). The used method is shown in 2.1. Different feature extraction methods are then used to derive characteristic values of the signal that allow the classification algorithm to distinguish between different movements.
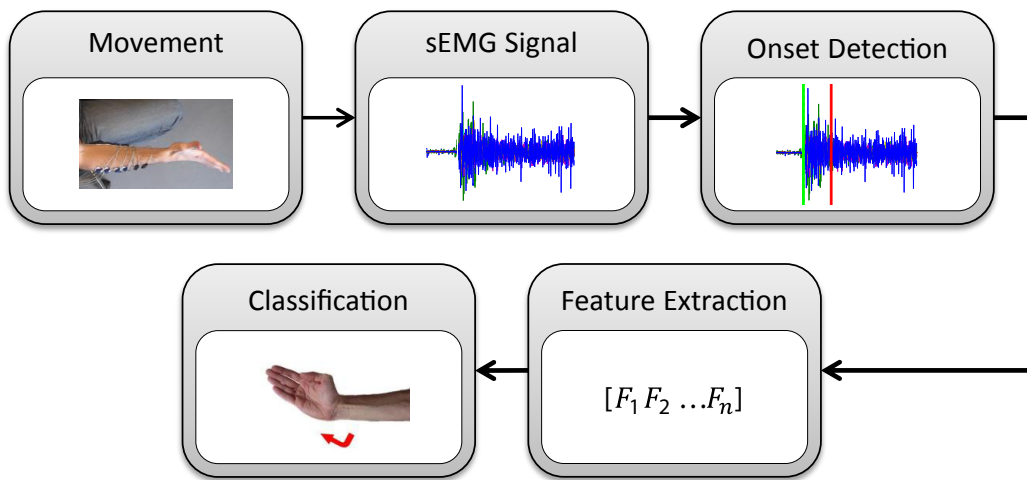
Figure 1.2: The concept of sEMG movement classification. The sEMG signal is recorded, an onset is detected, a segment defined by this onset and the feature length is used for feature extraction and these features are the used for classification of the performed movement.

1.1 The Electromyographic Signal

In order to successfully use the sEMG signal for the classification tasks one first has to understand the nature of this signal. The signal that is being used is the change of the motor unit action potential with respect to time. In order to measure useful signals one must have knowledge about the properties and the origin of sEMG signals, of the instruments used during signal measurement and basic understanding of the anatomy of the human muscular system in the region of interest. Only with this knowledge it is possible to recurringly acquire useful data for the given task.

In this section the reader will be given an overview of the mentioned topics. If the reader is interested in a more detailed description, references [15; 24] are to be considered.

1.1.1 Origin of the Myoelectric Signal

All the movements of our body are conducted by the various muscles that are connected to the joints via tendons. Whenever a movement is performed, action potentials are transferred from the motor cortex via the spinal cord and arrive at a motoneuron. Every muscle consists of a number of muscle fibers, which are grouped in several motor units. A motor unit is a group of muscle fibers that is controlled by a single α - motor neuron (Figure 1.3). These α - motor neurons are large (in case of diameter) motor neurons in the brain stem and the spinal cord that are heavily myelinated for higher transmission speeds. They innervate the muscle fibers of skeletal muscles via the neuromuscular junction and initiate the contraction.

When a muscle is activated, but before the contraction and the production of force starts, the exchange of ions across the membranes of muscle fibers generate small electrical currents [24]. The activation of the motor units depends on the required force of the contraction. For small forces only the small motor units are activated, whereas for larger forces larger motor units are being activated as well [36]. The electrical response of one particular motor unit is called the motor unit action potential (MUAP, Figure 1.4).

The actual shape of the action potential is influenced by the geometric properties of the muscle fibers (e.g. diameter, arrangement), the filtering effect of the tissue between the muscle and the electrode, as well as the properties of the recording electrode and the instrumentation [21]. Each electrode detects the sum of the electric signal of all the MUAPs in its detection area (or within a critical distance) and the recording of this signal over time is called the electromyogram. This is why the detected signal looks quite different than a single MUAP (Figure 1.5). In Figure 1.5 one can also observe the
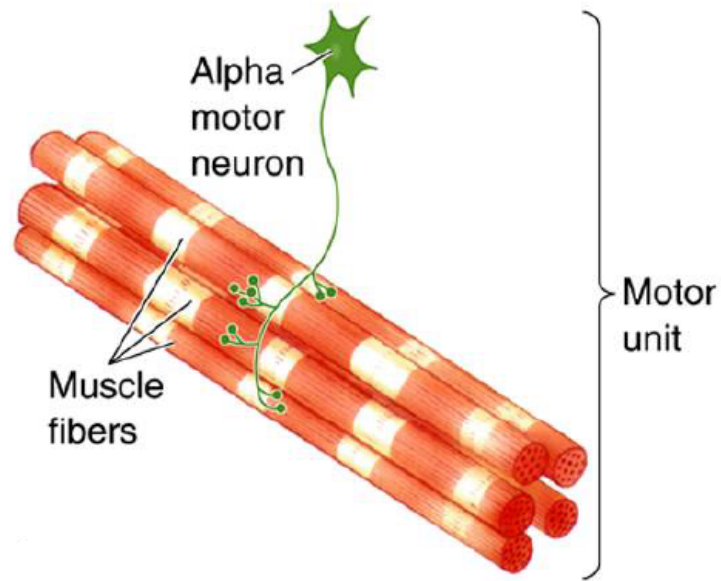
Figure 1.3: Illustration of a motor unit, modified from [6].
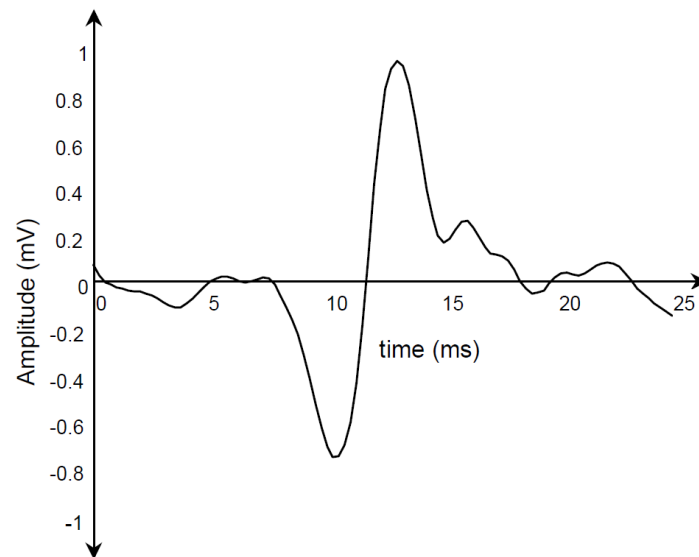
Figure 1.4: Typical motor unit action potential, adopted from [17].
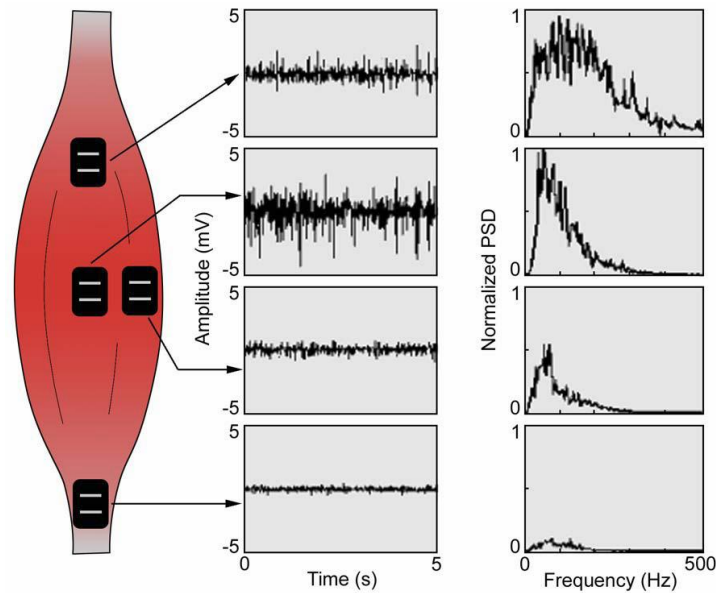
Figure 1.5: EMG Signals and their spectra as detected with the surface electrodes [16].

importance of proper positioning of the electrodes, that will be covered in chapter 1.2.2. It should be mentioned, that the sEMG signal can already be measured 10 to 100 ms prior to the output of mechanical force due to a process called "excitation-contraction-coupling" [24].

1.1.2 EMG Signal Properties

The surface electromyogram is a stochastic signal with an amplitude that is typically in the range from 0 to 6 mV (peak-to-peak) or 0 to 1.5 mV (RMS) [24]. The contributions of the sEMG signal outside the range of 5-10 Hz to 400-450 Hz are negligible [35]. Therefore it is very common to apply a bandpass filter to the signal (e.g. $f_{HP} = 5$ Hz and $f_{LP} = 500$ Hz).

The properties of the sEMG signal and its quality depend on several factors, such as the timing and intensity of the muscle contraction, the distance between the electrode and the active muscle area, the properties of the tissue between the electrode and the muscle (e.g. skin thickness, body fat), the properties of the hardware used for signal acquisition (i.e. the electrodes and amplifiers) and the quality and stability of the electrode-skin contact [15].

The first factor, the timing and intensity of the muscle contraction, is the relevant information for each of the muscles involved in the different movements, since the changes in these factors are what allow us to distinguish between the different movements using

the EMG signal.

The second factor is also very important. It is obvious that the distance between the electrode and the muscle area that should be recorded has a large impact on the quality of the measured signal. Hence it is crucial to know about the human anatomy in the region of interest and to place the electrodes properly, based on this knowledge.

The electrical properties of the tissue in between the electrode and the muscle are also very important. The impedance of skin tissue is generally higher than that of muscle tissue and therefore the skin tissue causes filtering of the EMG signal and the amplitude is decreased. Considering this, it is apparent that when measuring subjects with a higher impedance of the skin tissue (due to greater thickness or higher body-fat-percentage), correct placement of the measurement electrodes is even more important.

1.2 Methods of Recording

This section assesses the different recording techniques that are feasible to measure the sEMG signal.

1.2.1 Monopolar versus Bipolar Recording

There are two possible configurations for the electrodes:

- **Monopolar electrode configuration:** Here a single electrode is used to measure the sEMG signal against a reference electrode, which is placed on electrically unrelated tissue. This configuration has the disadvantage of not being able to filter signals from outside noise sources and also records signals from muscles in a relatively large distance to the electrode. However, this method has the advantage of greater simplicity and the smaller number of electrodes leads to a less bulky setup.

- **Bipolar electrode configuration:** This is the most common configuration for recording the sEMG signal. Here two separate electrodes are used to detect the signal of a single muscle, both with respect to a reference electrode. Then the two signals are subtracted from one another, hence eliminating signals that are the same for both electrodes, like 50/60Hz AC - signals from power lines or EMG signals from distant muscles. Unfortunately bipolar configurations act as a band-pass filter to the recorded signal, so that a smaller inter-electrode distance shifts the EMG bandwidth to higher frequencies and lowers the signal amplitude [24].

1.2.2 Electrode Placement

As already mentioned in 1.1.2, correct electrode placement is essential for the quality of the sEMG signal (see also Figure 1.5). The goal is to place the sensor at a location where a good and, equally important, stable sEMG signal can be acquired. The recommendation is to place the electrode in the middle between the distal motor end-plate (approximated by the muscle belly) and the distal tendon [15].

When using bipolar electrode configuration the conductive surfaces of the electrodes should be orientated parallel to the muscle fibers for optimal recording. [24]

The reference electrode, used to provide a common reference to the amplifier input, should be placed over an electrically neutral tissue [17]. The best way would be to place the reference electrode as far away as possible from the active muscles. However, this is often inconvenient, so the reference is often placed on a neutral tissue (e.g. bony prominence) near the target area.

1.3 Anatomy of the Human Forearm

In order to acquire viable signals from different muscles and subsequently classify different movements that are executed through exertion of these muscles a basic knowledge of the human anatomy in the region of interest is essential. In the following an overview of the anatomy of the human forearm will be provided. For more information, see [19; 32].

The Anterior Compartment

In the anterior compartment of the forearm the muscles are organized in three layers (superficial layer, intermediate layer and deep layer). These muscles are responsible for the flexion of the fingers, movements of the wrist and pronation. The superficial layer of the anterior compartment consists of the four muscles flexor carpi ulnaris, palmaris longus, flexor carpi radialis and pronator teres. In the intermediate layer only a single muscle - the flexor digitorum superficialis - is located. The three muscles flexor digitorum profundus, flexor pollicis longus and pronator quadratus are found in the deep layer. The three layers of muscles are illustrated in Figure 1.6 and their individual functions are listed in Table 1.1.

Muscle	Function
Superficial layer	
Flexor carpi ulnaris	Wrist flexion, ulnar deviation (adduction)
Palmaris longus	Wrist flexion
Flexor carpi radialis	Wrist flexion, radial deviation (abduction)
Pronator teres	Pronation
Intermediate layer	
Flexor digitorum superficialis	Flexion of the fingers
Deep layer	
Flexor digitorum profundus	Flexion of the fingers
Flexor pollicis longus	Flexion of the thumb
Pronator quadratus	Pronation

Table 1.1: Function of the muscles in the anterior compartment of the forearm. For more information, see [19, : Tables 7.10 – 7.12].

Figure 1.6: The three layers of muscles in the anterior compartment of the human forearm (right hand). The left image depicts the superficial layer of muscles, the middle image the intermediate layer and the right image shows the deep layer of muscles. This figure is modified from [19].

The Posterior Compartment

The posterior compartment of the forearm consists of two layers of muscles (superficial and deep) that are responsible for the extension of the fingers, movements of the wrist and supination. There are seven muscles located in the superficial layer of the posterior compartment. These muscles are the brachioradialis, the extensor carpi radialis longus, extensor carpi radialis brevis, extensor digitorum, extensor digiti minimi, extensor carpi ulnaris and the anconeus. Five muscles are located in the deep layer of the posterior compartment. These muscles are the supinator, abductor pollicis longus, extensor pollicis brevis, extensor pollicis longus and extensor indicis. The two muscle layers are shown in Figure 1.7 and the functions of the muscles are explained in Table 1.2.

Muscle	Function
Superficial layer	
Brachioradialis	Elbow flexion
Extensor carpi radialis longus	Wrist extension, radial deviation (abduction)
Extensor carpi radialis brevis	Wrist extension, radial deviation (abduction)
Extensor digitorum	Extension of the fingers
Extensor digiti minimi	Extension of the little finger
Extensor carpi ulnaris	Wrist extension, ulnar deviation (adduction)
Anconeus	Radial deviation during pronation, elbow extension
Deep layer	
Supinator	Supination
Abductor pollicis longus	Abduction & Extension of the thumb
Extensor pollicis brevis	Extension of the thumb
Extensor pollicis longus	Extension of the thumb
Extensor indicis	Extension of the index finger

Table 1.2: Function of the muscles in the posterior compartment of the forearm. For more information, see [19, : Tables 7.13 – 7.14].
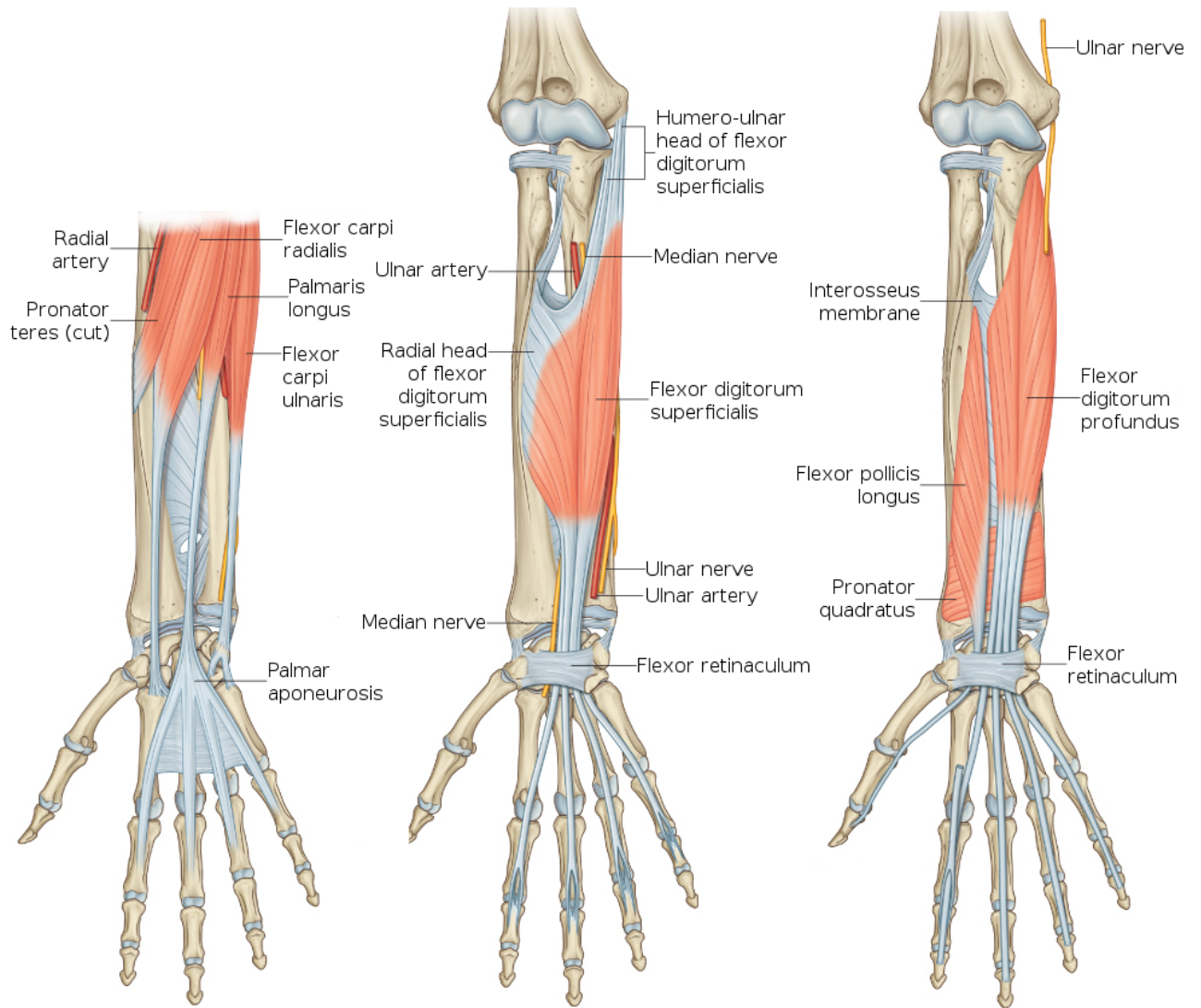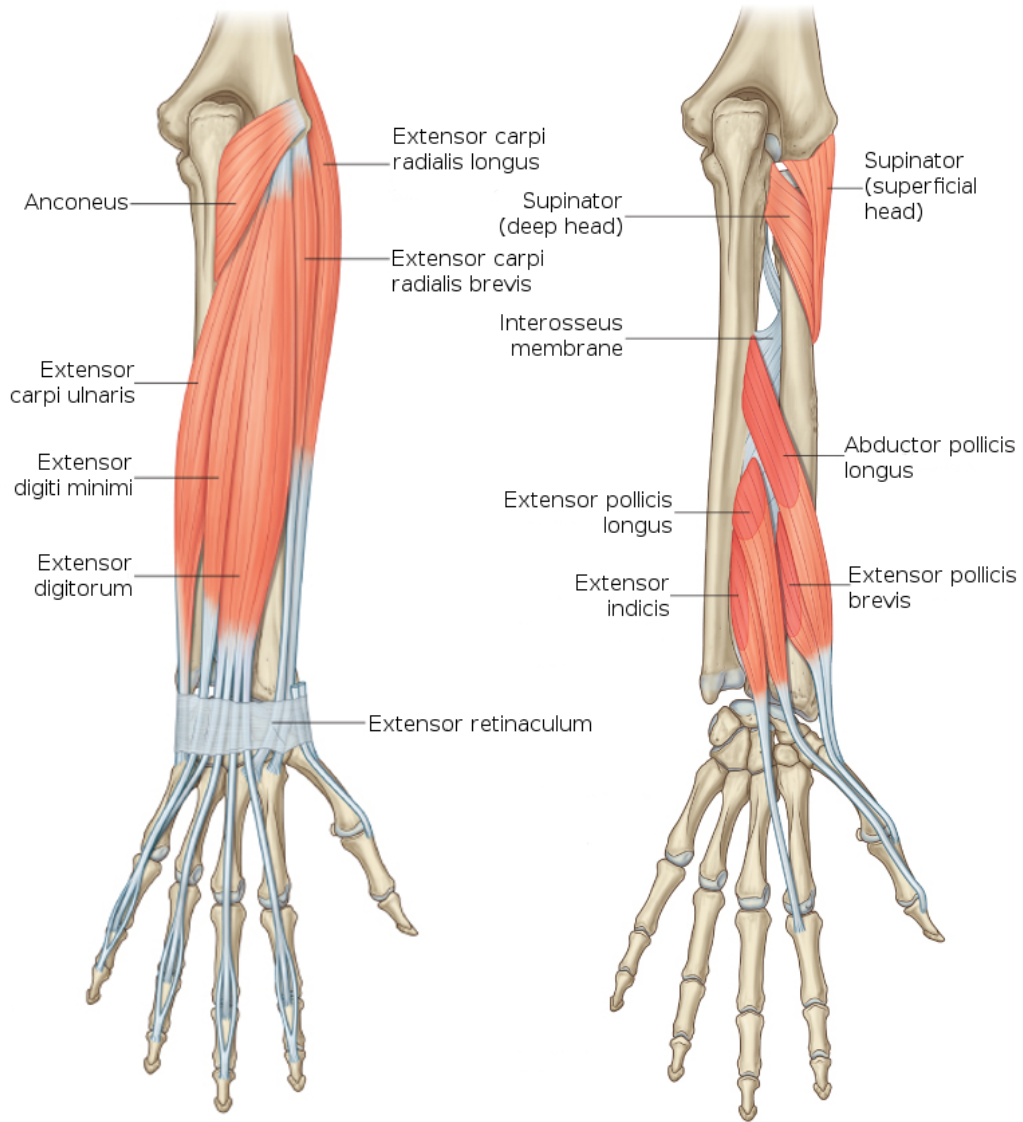
Figure 1.7: The two layers of muscles in the posterior compartment of the human forearm (right hand). The left image depicts the superficial layer of muscles and the right image shows the deep layer of muscles. This figure is modified from [19].

1.4 Motivation

As mentioned earlier, a reliable and robust online system for the classification of sEMG signals recorded from the forearm during different hand movements could be of great value to people that lost their hand due to an accident or some medical condition. While some of the robotic hands available today are already capable of restoring a great part of the functionality of the human hand, there is unfortunately still a lack of systems that are able to control all of the functions provided by these devices. Therefore the development of a robust, fast and accurate control algorithm based on the sEMG signals of the human forearm could help a lot of people that are handicapped by the consequences of an illness or an accident that led to a transradial amputation and is hence a goal worth striving for.

1.5 Goal

The goal of this thesis is to develop a system for the online classification of different hand and wrist movements. Based on literature research appropriate methods for signal recording and processing will be chosen. These methods will then be implemented in a real time system based on Matlab and Simulink. The implemented system should have a latency of below 300 ms and a good overall performance. Based on the results of an initial experiment with a number of different features, a good general feature set shall be derived and used for further experiments.

1.6 Organization of Chapters

Introduction

This section describes the motivation that lead to the realization of this thesis. It also gives an overview about the nature of the EMG signal and its acquisition as well as the basic anatomy of the muscles in the region of interest for this thesis (i.e. the forearm). Also, the goal of this thesis is described.

Fundamentals

Here, the methods that are commonly used for all of the experiments conducted in this thesis are described.

Feature Comparison Study

In this section the experiment conducted to investigate the performance of different features is described including the implemented feature extraction methods, the hard- and software used for the experiment, a detailed description of the experimental procedure as well as the results and a discussion of the results.

EMG Game Control

The implemented system has been applied to control a gaming application in a Human-Computer Interface scenario. The setup of the system and the experiment together with the gained results and the discussion of these results is provided in this section.

Hybrid System

In addition to the previous experiments the system has been used together with a Brain-Computer Interface in a hybrid system. The whole setup of this system is described in this section.

1.6.0.1 Discussion and Conclusion

This thesis is concluded by a discussion of some general aspects that have not already been addressed in the discussion sections of the individual experiments. Some possible directions and improvements for future work are also presented.

2 Fundamentals

This section will give an overview of the commonly used methods for all the experiments of this thesis.

2.1 Onset Detection

The first very important step in the processing of the sEMG signal is the correct detection of the beginning of a movement. Often the initial parts of the signal during the execution of a movement are the most significant when it comes to the classification of this movement. Hence it is very important not to miss these initial MUAPs due to a belated onset detection. A premature detection of an onset on the other hand would lead to the recording of data without valuable information about the movement performed. This would not only add noise to the feature extraction performed later on, but also precious information would be lost because the time window available for feature extraction in an online sytem is limited in order to keep latency low. Most of the algorithms for onset detection consist of some sort of signal conditioning, a detection unit whose output is an 'alarm' when an onset is detected and a post-processor that checks these alarms for their relevance.

Staude et al. in 2001 [51] compared several methods for onset detection, both threshold-based and statistically enhanced. They came to the conclusion that the statistically enhanced methods generally promise a better performance, but they are also tainted with greater complexity and computational effort, which could be hindering in an online classification system. Hence it has been decided that one of the more simple threshold-based approaches will be used for the design of the online system in this thesis. Among the threshold-based methods that have been compared in [51], the method implemented by Bonato et al. [9] performed best when real sEMG data has been used for the evaluation. Also, the performance of the Bonato method came closest to the statistically enhanced methods ([51, Table 3]). These results suggest that the Bonato method is well suited for the task at hand and hence it will be used for this thesis.

2.1.1 Method by Bonato et al.

The algorithm for this method consists of a test function that outputs an alarm if an onset candidate is found in any of the recorded channels and a post processing unit that checks these alarms for their relevance. The test function for this algorithm is given by:

$$g_k = \frac{1}{\hat{\sigma}_0^2} \left(y_{k-1}^2 + y_k^2 \right)$$

As can be seen, the decision function sums up the squares of two successive samples of the EMG signal and divides that sum by σ_0^2, which is the variance of the first M samples of the EMG signal, where no movement should be performed (i.e. the variance of the resting state). In the Bonato method the test function is only evaluated for odd k's. The decision rule for an alarm is a simple comparison of g_k for these k's to a given threshold h.

$$t_a = min\{k = 1, 3, 5, \ldots : g_k \geq h\}$$

The post processing stage consists of two rules and the alarm is only accepted if both of them apply. These rules are:

- at least n out of m samples must exceed the threshold h in order to indicate an active state

- such an active state has to be at least T_1 samples long.

If this check is positive, then the earliest beginning of this active state is taken as $\hat{t}_0$, the estimate for the onset time.

The parameters n, m and T_1 for the Bonato method are chosen in the same way as in [51] with: $n = 1$, $m = 5$ and $T_1 = 50$. The threshold h has been determined iteratively. The value has been varied and the algorithm has been applied to a data set of 60 executions of ten different movements (6 per movement). The result of the onset detection has then be inspected together with the underlying sEMG signal. Since the sEMG is a rather strong signal, the visual determination of the onset of movement from a resting position is relatively easy. The threshold has then be adapted in such a way that the onset found by the algorithm was closest to the visually determined onset for all of the movements. This resulted in choosing a value of $h = 300$ for the threshold for all of the channels.

2.2 Support Vector Machines

SVMs are a popular tool for the classification of EMG signals among a number of researchers [33; 38; 45; 59]. Oskoei and Hu in 2008 [38] have compared SVMs to linear discriminant analysis (LDA) and multi layer perceptron (MLP) neural networks. Their findings regarding the SVM were that "It demonstrates exceptional accuracy, robust performance, and low computational load" [38]. This encourages the use of a SVM for the task at hand.

In the next sections some theory about binary SVM and their expansion for multiclass problems will be provided. For further information, the reader is pointed to [26; 55]

2.2.1 SVM - Theory according to [26]

Support Vector Machines represent the pairs of training data $\mathbf{x}$ and corresponding class labels $\mathbf{y}$ through vectors in a vector space. The SVM then tries to fit a hyperplane into this vector space that separates the training points into two different classes. Because there are often many different hyperplanes that could separate the training data the SVM tries to achieve maximum separation between the classes or to maximize the distance between the decision boundary and the nearest data point on each side. This distance is called the margin. The hyperplane that can be seen in Figure 2.1 is defined by (2.1)

$$\{x : f(x) = x^T \beta + \beta_0 = 0\} \tag{2.1}$$

In this equation, the variable β is a unit vector, i.e. $\|\beta\| = 1$. The separation of the data into the two classes can then be done by simply calculating the sign of the output of this equation, as given in (2.2).

$$G(x) = sign[x^T \beta + \beta_0] \tag{2.2}$$

Now there are two possibilities concerning the data:

1. The classes are linearly separable

2. The classes overlap in feature space

17
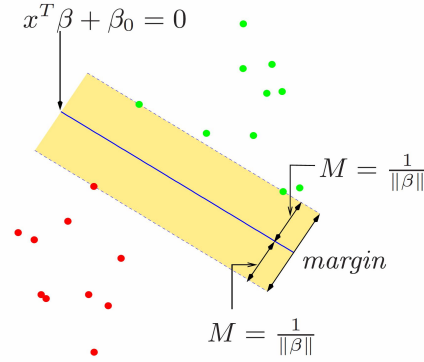
Figure 2.1: Decision boundary in the separable case, from [26]. The solid line is the decision boundary, the broken lines indicate the maximal margin of width $2M = 2/\|\beta\|$.

Ad 1:

When the classes are separable, it is possible to find a hyperplane that creates the biggest margin between the data points of the different classes. The search for the biggest margin is an optimization problem that is given by (2.3)

$$\max_{\beta,\beta_0,\|\beta\|=1} M$$
$$\text{subject to } y_i(x_i^T\beta + \beta_0) \geq M, \ i = 1, \ldots, N \tag{2.3}$$

The constraint of β being a unit vector can be dropped by replacing the conditions with:

$$\frac{1}{\|\beta\|} y_i \left(x_i^T\beta + \beta_0\right) \geq M, \tag{2.4}$$

where β_0 is redefined, or

$$y_i \left(x_i^T\beta + \beta_0\right) \geq M\|\beta\|. \tag{2.5}$$

Now $\|\beta\|$ can be arbitrarily set to $1/M$. This is due to the fact that for any β and β_0 satisfying the inequalities, any positive multiple satisfies them too. Because of this, the optimization problem can be simplified to (2.6)

$$\min_{\beta,\beta_0} \|\beta\|$$
$$\text{subject to } y_i(x_i^T\beta + \beta_0) \geq 1, \ i = 1, \ldots, N \tag{2.6}$$

Where $M = 1/\|\beta\|$. So the norm of β is minimized with respect to the fact that the class

label prediction and the true class label have to be on the same side of the hyperplane $(y_i \cdot f(x_i) \geq 1)$.

Ad 2:

If the classes given by the training data overlap in the (original) feature space there are again two ways of how to deal with it:

a) Still maximize M, but allow errors

b) Enlarge the feature space by using basis expansions

Ad a:

To allow errors means to accept that some of the training points to lie on the wrong side of the decision boundary. Therefore one introduces slack variables $\xi = (\xi_1, \xi_2, \ldots, \xi_N)$. An illustration of the non-separable case with slack variables can be found in Figure 2.2
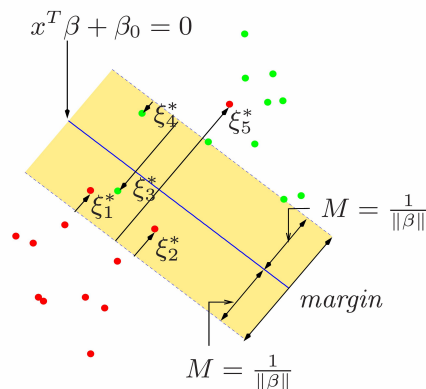
Figure 2.2: Decision boundary in the non separable case with slack variables, taken from [26]. The solid line is the decision boundary, the broken line indicates the maximal margin. Points labeled with ξ_j^* are on the wrong side of their margin.

Now the constraint for the optimization problem in (2.3) can be modified in two different ways:

$$y_i(x_i^T\beta + \beta_0) \geq M - \xi_i \tag{2.7}$$

or

$$y_i(x_i^T\beta + \beta_0) \geq M(1 - \xi_i) \tag{2.8}$$

Where $\xi_i \geq 0 \,\forall i$ and $\sum_{i=1}^{N} \xi_i \leq$ some constant. The two choices (2.7) and (2.8) lead to different solutions of the problem. While (2.7) measures the overlap of the data point as the absolute (or actual) distance from the margin, (2.8) measures the overlap as the relative distance that changes when the width of the margin M changes. But the important thing is that (2.7) leads to a non convex optimization problem, whereas (2.8) leads to a convex optimization problem, which has the advantage that if a local minimum exists, it is *always* a global minimum.

The idea of the slack variables is that ξ_i in (2.8) is the proportional amount by which the prediction based on x_i $(f(x_i) = x_i^T\beta + \beta_0)$ is on the wrong side of its margin. So bounding the sum $\sum \xi_i$ to an upper value bounds the number of errors on the training set to the given value. In the algorithm the optimization with slack variables is given by:

$$\min\|\beta\| \text{ subject to } \begin{cases} y_i(x_i^T\beta + \beta_0 \geq 1 - \xi_i \,\forall i \\ \xi_i \geq 0, \; \sum \xi_i \leq C \end{cases} \tag{2.9}$$

Where C is the "cost parameter". The optimal value for C can be found via cross-validation.

Ad b:

Enlarging the feature space with basis expansions, such as polynomials or radial basis functions, leads to a more flexible classifier. This is because linear boundaries in the enlarged feature space transform to nonlinear boundaries in the original feature space and generally achieve better separation of the classes. The difference to the case before is that instead of using x_i for the estimation, now the transformed feature vectors $h(x_i) = (h_1(x_i), h2(x_i), \ldots, h_M(xi))$ are used. Using this expansion, the input dimension is allowed to get very large. But since h(x) appears in both the optimization problem and the solution function $(f(x))$ through inner products, one does not need to explicitly define $h(x)$ at all. All that is needed for the calculation is knowledge of the kernel

function (2.10) that computes the inner product in the transformed space.

$$K(x, x') = \langle h(x), h(x') \rangle \tag{2.10}$$

Popular choices for K are:

- Polynomial function of degree d: $K(x, x') = (1 + \langle x, x' \rangle)^d$

- Radial Basis Functions: $K(x, x') = e^{-\gamma \|x - x'\|^2}$

- Neural network : $K(x, x') = \tanh(\kappa_1 \langle x, x' \rangle + \kappa_2)$

In this enlarged feature space the cost parameter has the following role: A large value for C will lead to overfitting while a smaller value for C will lead to a smoother decision boundary in the original feature space. So C controls the upper boundary of the Vapnik Chervonenkis- (VC-) dimension. In the case of (the frequently used) Radial Base Functions the second parameter γ describes the width of the gaussian bell curve. Two examples of nonlinear decision boundaries in the original feature space can be found in Figure 2.3.

SVM - Degree-4 Polynomial in Feature Space

Training Error: 0.180
Test Error: 0.245
Bayes Error: 0.210

SVM - Radial Kernel in Feature Space

Training Error: 0.160
Test Error: 0.218
Bayes Error: 0.210
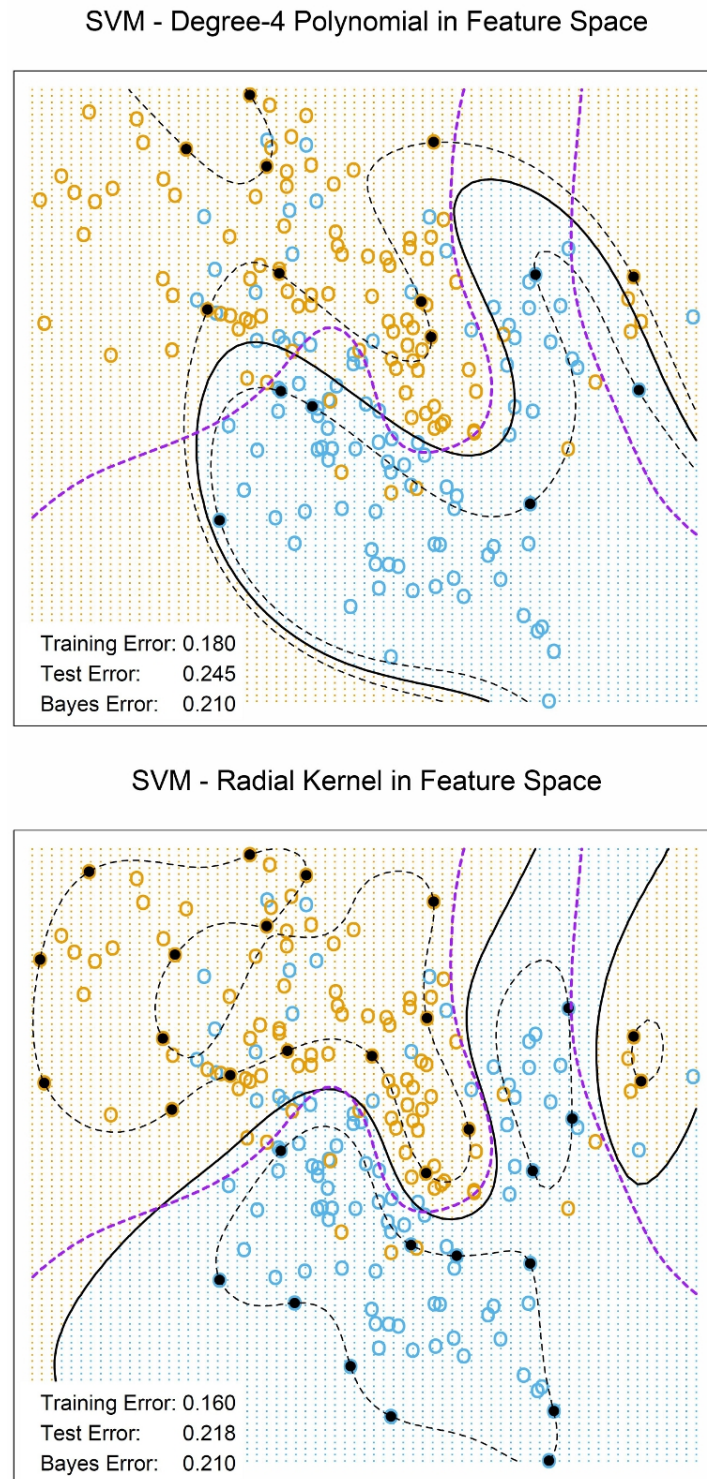
Figure 2.3: Two nonlinear Support Vector Machines, taken from [26]. The upper plot shows the decision boundary using a 4th-order polynomial kernel, the lower plot uses a radial basis kernel with $\gamma = 1$. The broken purple line in both plots is the decision boundary of the bayes classifier.

2.2.2 Expansion for Multiclass-Problems

Since a support vector machine is a binary classifier, some adaptations have to be done in order to solve classification problems with more than two classes. There are several methods to modify the classification to handle more than two classes (according to [4] and [28]):

- **One-against-all (OAA) classification** where there is one binary SVM for each class, and the SVM for each is trained with all data of this class with positive labels and all data of the other classes with negative labels. The classification result in this case is determined via a voting process. As can be seen in Figure 2.4, using binary decision boundaries in this case can be problematic because this can result in regions in the feature space that can not be classified. In other words a data point can only be classified under a certain class if the SVM of that particular class votes positive and the SVMs of *all other* classes vote negative. To avoid this, instead of using only the signs of the decision functions of the SVMs and hence using binary decision boundaries one has to use the continuous values of the decision function and assign the data point the label of the class that achieves the highest value of the decision function. An illustration of this can be seen in the middle of Figure 2.4

- **One-against-one method (Pairwise Classification)** where for a classification Problem with N classes $N(N-1)/2$ classifiers are constructed, each one for a pair of classes and all these classifiers are trained with data from the two classes. The classification is conducted via a voting process, where the data is then assigned the class label of the class with the most 'wins'.

- **Multiclass ranking SVMs** where one single mathematical decision function is sought that can distinguish between all the different classes.
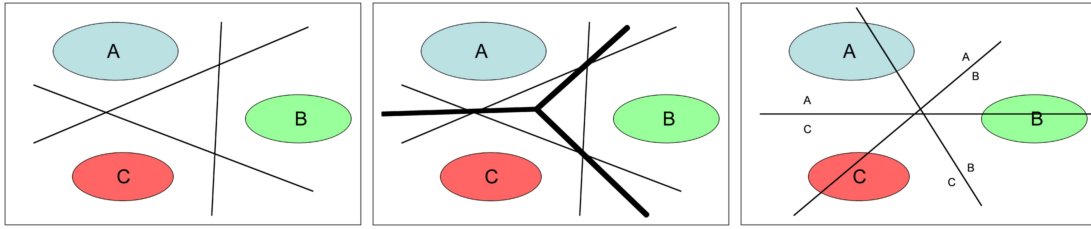
Figure 2.4: Decision boundaries of different methods for multiclass SVMs, adopted from [4]. The left picture shows the decision boundary of a OAA method with binary decision boundaries for a three class problem. Note that the region in the middle can not be classified. The middle picture shows the same problem for a OAA classifier with continuous decision boundaries, where the problem of regions that can not be classified is avoided. The right picture shows the decision boundaries of the $N(N-1)/2$ classifiers used for the pairwise classification method.

2.2.3 SVM used for this Thesis

There are a lot of SVM implementations that are ready to use available on the internet. The package used for the work in this thesis is LIBSVM [14]. LIBSVM provides several different SVM approaches, has a built-in function for cross validation in order to conduct model selection and contains various kernels that can be used. It also provides the possibility to get the probability outputs for each class in order to get some sort of "confidence measure" in addition to the classification result. For multiclass problems LIBSVM implements the one-against-one method as described earlier. For this work, a classification SVM Type 1, or C-SVM classification as described in 2.2.1 with a radial base function kernel has been used. This kind of SVM has two tunable parameters, the cost factor C and the kernel parameter γ. The ideal values for these parameters are found in the model selection phase by performing a grid search.

2.3 Cross Validation

Cross validation (CV) is a method that is commonly used for the evaluation of a classifiers performance and for model selection. In this thesis a 10 x 10 cross validation will be used. This means that the training data is split up into 10 stratified subsets and in ten different runs, each of the subsets is once used for testing while the other 9 sets are used for training the classifier. This process is then repeated 10 times and a mean accuracy is calculated. For more information the reader is pointed to [7].

2.4 Confusion Matrix

A confusion matrix is used to visualize the performance of a learning algorithm. It is a matrix of size $n \times n$ where n is the number of classes. The rows of the matrix represent the true class labels and the columns represent the class labels that were predicted by the algorithm. The ideal confusion matrix is a unit matrix. Off-diagonal elements represent misclassifications. The confusion matrix helps to find out if one class is commonly predicted as another and thus provides more information than the plain classification accuracy in a multiclass problem.

2.5 Analysis of Variance

The analysis of variance (ANOVA) is a statistical method that, as the name suggests, calculates the variance of the tested quantities to analyze whether the means of different data groups are the same or if there is a statistically relevant difference between one or more of the groups. The null-hypothesis of the ANOVA is that the means of all the data groups are the same. If the null-hypothesis is rejected, then a post-hoc test has to be conducted in order to find out which of the groups are significantly different. In this thesis a univariate ANOVA is used in combination with a Newman-Keuls test. More information about statistical analysis can be found in [11].

3 Feature Comparison Study

The first goal of this thesis was to assess the quality of different features that can be derived from the recorded sEMG signals with respect to their cross validation performance on the recorded training data. The performance of the different features across all ten subjects should then be examined to evaluate the general performance of the individual features. Based on the results of the feature comparison for each individual subject the best feature for the respective subject should be chosen and used in an online classification task to test the performance of the system. The conducted experiments and the used methods for these tasks are described in this section.

3.1 Signal Recording Hardware

3.1.0.1 Electrodes

For this experiment adhesive, disposable Ag/AgCl electrodes Kendall™ Arbo™ H124SG have been used to acquire the sEMG signals of the forearm muscles. A datasheet of these electrodes can be found on the internet [1]. The preparation of the skin consisted of cleansing the skin thoroughly with alcohol without shaving the arm or using some sort of abrasive gel. This procedure was chosen since the focus of this thesis was to develop a system for possible daily use and hence preparation time and subject discomfort was kept to a minimum.

3.1.0.2 Biosignal amplifier

A single g.USBamp biosignal amplifier from g.tec (Guger Technologies OEG, Graz, Austria, www.gtec.at) was used to record the EMG signals from the 16 surface electrodes. The properties and frequency range of the EMG have already been assessed in 1.1.2 where it has been stated that it is very common to apply a bandpass filter to the signal. The g.USBamp biosignal amplifier comes with built-in filters that can be adjusted to predefined values. For this thesis the cutoff frequencies of the high pass and the low pass filters are set to $5\,\mathrm{Hz}$ and $500\,\mathrm{Hz}$, respectively. The filter type for both filters was Chebyshev and the order of the filters was 8. The notch filter to cancel out power line interference has always been turned on and the sampling frequency was $2400\,\mathrm{Hz}$ for all measurements.

3.2 Software

For this thesis Matlab® and Simulink® (MathWorks, Natick, Massachusetts, U.S.A., www.mathworks.com) were used for all the signal acquisition and signal processing steps as well as for presenting the paradigms. Features from the BioSig toolbox [48] were used within Matlab.

The data was stored in the "General Data Format" (.gdf - File) [49].

3.3 Implemented Feature Extraction Methods

The acquisition of a set of one or more different features is a very important step in the classification process based on the EMG signals. The feature set should be chosen in a way that the most important properties of the underlying data set are accurately described while the amount of data should be kept small. There are many different approaches for feature extraction from EMG signals. It is possible to extract features from the time domain, the frequency domain or the time-frequency domain. In this chapter the reader will be given an overview of the feature extraction methods implemented for this thesis.

3.3.1 Time Domain Features

The feature extraction methods in the time domain are generally easy to implement and computationally inexpensive which is a desirable characteristic for the online application. They are also small and therefore allow to combine several features to a more powerful feature vector. Dependent on the task at hand, time domain features may even outperform more complex feature extraction methods, as, for example, shown in [20]. There are numerous approaches of time domain features in literature. An excerpt of these is used for this thesis and described here.

3.3.1.1 Mean Absolute Value (MAV)

This feature simply calculates the mean value of the rectified EMG signal x_n in a time window with N samples [61]. It is calculated by:

$$\text{MAV} = \frac{1}{N} \sum_{n=1}^{N} |x_n|$$

3.3.1.2 Slope Sign Changes (SSC)

The Slope Sign Change feature is related to the signal frequency. SSC counts the number of times that the slope of the signal waveform changes its sign. To avoid unnecessary noise a threshold is used to check the changes for their relevance. The formula for the calculation is given by [41]:

$$\text{SSC} = \sum_{n=2}^{N-1} f\left[(x_n - x_{n-1}) \cdot (x_n - x_{n+1})\right],$$

$$\text{where} f(x) = \begin{cases} 1, \text{if } x \geq threshold \\ 0, \text{otherwise} \end{cases}$$

where x_n is the nth sample of the EMG signal.

3.3.1.3 Variance of the EMG (VAR)

The EMG signal can be modeled as white gaussian noise with a dynamic variance σ^2 [51]. Hence, the variance of the EMG signal is a measure of its power [61] and can be used to distinguish between different movements.

3.3.1.4 Waveform Length (WL)

The waveform length is the cumulated length of the signal waveform in the inspected segment. The waveform length is related to the amplitude of the signal, its frequency and the time [41]. It is calculated by summing up the absolute differences between two successive data points of the EMG signal x_n:

$$\text{WL} = \sum_{n=1}^{N-1} |x_{n+1} - x_n|$$

3.3.1.5 Willison Amplitude (WAMP)

This feature calculates the times that the difference between two consecutive samples of the EMG signal exceeds a certain threshold [61]. It is an indicator of firing of motor unit action potentials which is related to the muscle contraction level [61]. The formula to calculate the WAMP is given by:

$$\text{WAMP} = \sum_{n=1}^{N-1} f\left(|x_n - x_{n+1}|\right)$$

$$\text{where} f(x) = \begin{cases} 1, \text{if } x \geq threshold \\ 0, \text{otherwise} \end{cases}$$

The value for this feature is determined by the number of times the absolute value of the difference between to consecutive samples of the EMG signal x exceeds a certain threshold.

3.3.1.6 Histogram of the EMG (HIST)

For this feature introduced by Zardoshti-Kermani et al. in 1995 [60] and also reviewed by Tkach et al. in 2010 [54], the amplitude range of the EMG signal is divided into a number of bins and the number of data points that fall into the respective bins is calculated. This feature has a higher dimension than the other time domain features used in this work (i.e. #bins · #channels).

3.3.1.7 Simple Square Integral (SSI)

The simple square integral, as the name suggests, is the integral of the squares of all the data points in the observed time segment. It is calculated by:

$$\text{SSI} = \sum_{n=1}^{N} x_n^2$$

Where x_n is the nth data point of the EMG signal that is N samples long.

3.3.1.8 Log-Detector (LD)

The log-Detector feature is related to the muscle force [60]. The Feature is defined by:

$$\text{LD} = e^{\frac{1}{N} \sum_{n=1}^{N} log(|x_n|)}$$

Again, x_n represents the nth sample of the EMG signals consisting of N samples.

3.3.2 Frequency Domain Features

3.3.2.1 Median Frequency (MDF)

For this feature the spectrum of the EMG signal is calculated via Fast Fourier Transform (FFT). The MDF is defined as the frequency at which the area under the spectrum curve (i.e. the integral) is divided into two equal parts [41]. To calculate the spectrum the signal has been zero padded to the next integer power of two and a hamming window has been applied. The median frequency can be defined via the following equation:

$$\sum_{n=1}^{\text{NMDF}} S_n = \sum_{n=\text{NMDF}}^{N} S_n = \frac{1}{2} \sum_{n=1}^{N} S_n$$

Where S_n is the amplitude at the *nth* frequency bin of the spectrum consisting of N bins and NMDF is the frequency bin of the median frequency.

3.3.2.2 Mean Frequency (MNF)

The second feature based on the spectrum of the EMG is the mean frequency. The steps to calculate the spectrum were the same as for MDF. The feature is calculated as the weighted sum of the spectrum divided by the total sum of the spectrum [41]. It is defined by:

$$\text{MNF} = \frac{\sum\limits_{n=1}^{N} f_n S_n}{\sum\limits_{n=1}^{N} S_n}$$

Where S_n denotes the amplitude of the spectrum at a certain frequency bin n.[41]

3.3.3 Feature Parameter Selection

Some of the presented features have tunable parameters. The Features WAMP and SSC have a threshold value that can be adapted while for HIST, the number of bins can be adjusted. The threshold values have been found by evaluating the performance of the (single) features on a data set with 10 classes and 120 trials in total. This data set has been divided into a training set and a test set of equal size. The threshold values have then been optimized to gain optimal performance on the test set. This resulted in the usage of threshold value of $30\,\mu\text{V}$ for WAMP and $100\,\mu\text{V}^2$ for SSC. For HIST, the number of bins has been set to a fixed value of 9 to have results that are comparable to [54]. The bins have been spaced equally between the minimum and maximum voltage of the recorded signals.

3.3.4 Segment Length for Feature Extraction

As already mentioned, the goal is to keep the latency of the system small. In order to keep the time between a movement and a classification result below $300\,\text{ms}$, a segment length of $250\,\text{ms}$ has been chosen. This leaves $50\,\text{ms}$ for feature extraction and classification. The absolute execution time of the implemented method has been investigated in order to make sure that this goal is fulfilled. On the machine used for this work (Intel i5-2500K @3.3 GHz, 8GB RAM), none of the S-Functions for feature extraction implemented in Simulink took longer than $1\,\text{ms}$ for execution and the SVM classlabel prediction took a similar timespan. These times were measured with the built-in Matlab functions 'tic' and 'toc'.

3.4 Experimental Procedure

This next section provides information about the different aspects of the experiment procedure including the movements chosen for the classification problem, the placement of the electrodes and information about the subjects and the different phases of the experiment.

3.4.1 Movements to Classify

In order to evaluate the performance of the online system a number of gestures has to be defined that should be classified. For this thesis it has been decided to aim for classifying 10 different movements against each other based on the sEMG signals of the proximal part of the forearm. The following list presents those chosen movements and the abbreviations used in the results section:

- Flexion and extension of the wrist (W.E. and W.F.)

- Wrist deviation ulnar and radial (D.U. and D.R.)

- Pronation and supination (Pro. and Sup.)

- Making a fist (Fi.)

- Extension of all fingers (E.A.)

- Extension of the thumb (Th.)

- Pinch grasp (Pi.)

These movements have already been mentioned in 1.3 where the relationship between the individual muscles and the movements has been explained (see Tables 1.1 and 1.2). The muscles for the recording of the sEMG have been chosen based on this knowledge.

3.4.2 Electrode Placement

As already mentioned, the electrodes for this thesis should be placed on the proximal part of the forearm. This is necessary to have a system that is also suitable for transradial amputees since electrodes on the distal part of the forearm or even the hand are not applicable in this case. The electrodes to record the EMG signals during the movements mentioned above were placed over the following muscles of the subjects right forearm (Figure 3.1):

- M. flexor carpi radialis

- M. flexor carpi ulnaris

- M. flexor pollicis longus

- M. extensor carpi radialis longus

- M. extensor carpi radialis brevis

- M. extensor carpi ulnaris

- M. extensor digitorum

- M. extensor pollicis longus
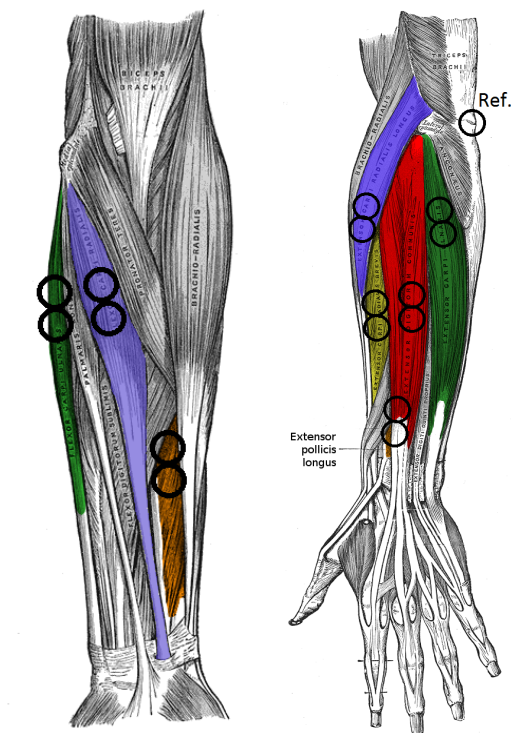
Figure 3.1: Illustration of the muscles that were used for the acquisition of sEMG signals. The images show the anterior and posterior side of a left human forearm. The left image shows the anterior side with the flexor carpi radialis (blue), the flexor carpi ulnaris (green) and the flexor pollicis longus (orange). The right image shows the extensor carpi radialis longus (blue) and brevis (yellow), the extensor carpi ulnaris (green), the extensor digitorum (red) and the extensor pollicis longus (orange, in the deep layer - see label). Both images are modified from [23].

A pair of electrodes was placed over each muscle belly in order to calculate a bipolar derivation. The location of the muscle belly was felt out during the execution of movements to exert the muscles of interest. The reference electrode was placed on the elbow since firstly this is a very prominent bone and secondly it is close to the region of interest on the forearm.

3.4.3 Subjects

The experiment has been conducted with a total of 10 subjects. Four of the subjects were female, six male, and the mean age was 31.1 years. One of the subjects was left-handed. This has not been a reason for exclusion from the experiment or for placing the electrodes on the other arm, since for the application in prosthetics the implemented system should also work with the non-dominant hand, of course.

3.4.4 Phases of the Experiment

The whole test consisted of a preparation phase, a training session and a testing session. Between each of these steps a questionnaire with visual analog scales (VAS) was used to assess the users comfort and muscle fatigue. The VAS used in the questionnaire was 10 cm long so the score ranged from 0 (worst) to 10 (best). An illustration of the whole experimental procedure can be found in Figure 3.2. An example of the used VAS is shown in Figure 3.3.
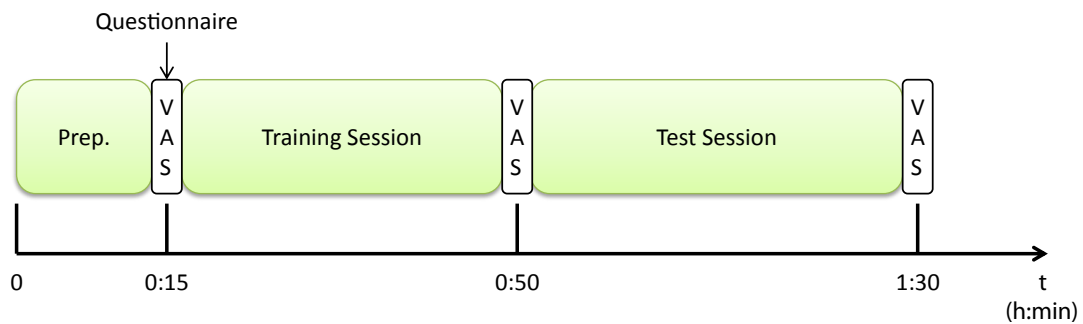
Figure 3.2: Illustration of the experimental procedure consisting of a preparation phase of approximately 15 minutes duration followed by the training and test session. After each of these steps the subjects filled out a questionnaire with VAS.

Wie empfinden Sie die Elektroden auf Ihrem Arm?

0 = äußerst ●————————————————————————————● 10 = nicht
störend   störend

Fühlen Sie eine Erschöpfung Ihrer Unterarmmuskulatur?

0 = äußerst ●————————————————————————————● 10 = nicht
erschöpft   erschöpft

Figure 3.3: Example of the VAS used in the questionnaire.

Preparation Phase

During the preparation phase the whole experiment has been explained to the subjects. They were shown the cue images and a demonstration of the upcoming paradigm without data recording has been performed. During this introduction the electrodes have been placed on the subjects forearm. After the subjects understood the procedure of the experiment they all signed an informed consent form. Also, the derived signals have been inspected visually by a scope. After this, a resting file of approximately $10\,\text{s}$ length has been recorded where the subjects were asked not to perform any movements and keep their hand in the resting position. This was necessary to calculate the rest variance from $400\,\text{ms}$ of data that is used in the test function of the Bonato onset detection algorithm. The 400ms of data have been extracted beginning after $3.5\,\text{s}$ after the beginning of the file.

Training Session

The training session consisted of a total of four training runs with 70 trials each (i.e. 7 per class). Each of these runs took about six minutes. The runs were controlled by a paradigm that is illustrated in Figure 3.4. A single trial consisted of:

- An initial beep

- A break of 0.75s duration

- 1.5 s where one of the 10 cues is displayed in pseudo-random order and the subjects should perform the indicated movement

- A random break of 2 to 3.5 seconds duration

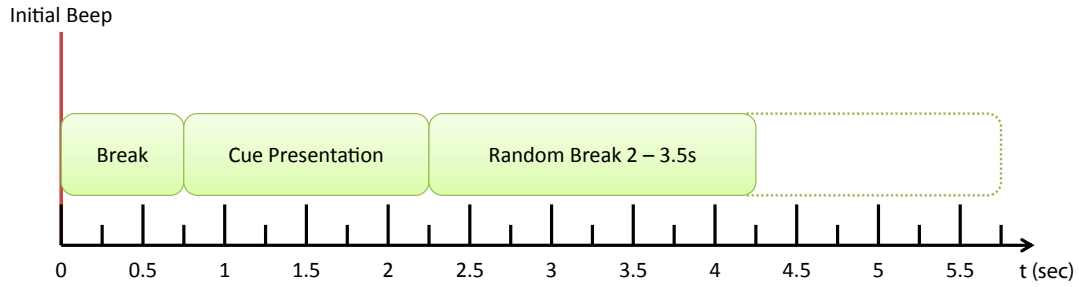The cue images for the chosen movements are shown in Figure 3.5.

Figure 3.4: Illustration of a single trial of the paradigm used to control the training session. Each trial consists of an initial beep, a break of 750 ms, 1.5 s of cue presentation and a random pause of 2 s - 3.5 s.
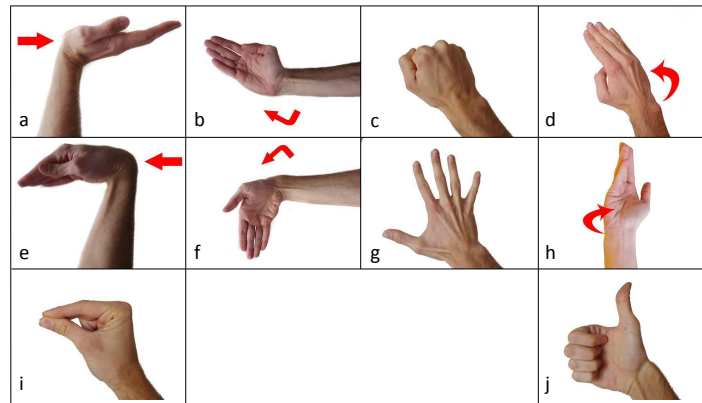

Figure 3.5: The different cue images that were shown to the subjects. Wrist extension (a), radial deviation (b), fist (c), pronation (d), wrist flexion (e), ulnar deviation (f), all fingers extension (g), supination(h), pinch grasp (i), and thumb extension (j).

After the 280 training trials have been recorded, the onset detection algorithm has been used to find the beginning of the movement in each of the trials. The investigated data segment were the 1.5 s during cue presentation. The first index at which an active state in any of the 8 bipolar channels was detected was then used as the beginning of the 250 ms data segment for the 10 different feature extraction methods. The resulting features have then been normalized to a range of -1 to 1 and these normalized features were used to train the support vector machine. This training consisted of two steps.

In the first step, the ideal parameters C and γ for the SVM have been determined by using a grid search and 10×10 cross validation for each feature separately. This grid search has been performed in the range $[C = 2^c | c = 2 \ldots 11]$ and $[\gamma = 2^g | g = -6 \ldots 2]$ with integer values for c and g. This step size has been chosen to find the optimal parameters, or at least parameters close to the optimal value, in a reasonable amount of time. The best cross validation result for each feature and the respective parameters

have been stored and in the second step, only the best feature for the respective subject has been used to train the classifier for the test session.

Test Session

The paradigm that controlled the trials during the test session was very similar to that of the training session. Again, the subject was presented a cue image in pseudo-random order. The only difference was that in this run the subject was provided with acoustic feedback during the cue presentation time. A Matlab-S-Function looked for new classifications within the presentation time and if the result of the online classification matched the class that was related to the cue image a tone with a frequency of 1000 Hz and a duration of 0.6 s was played. If the classes did not match a tone with a frequency of 330 Hz was played. An illustration of the paradigm can be found in Figure 3.6. The complete test session consisted of 4 runs with 80 trials each, so a total of 320 trials (32 trials per class) has been recorded. Each of these runs took about 7 minutes.
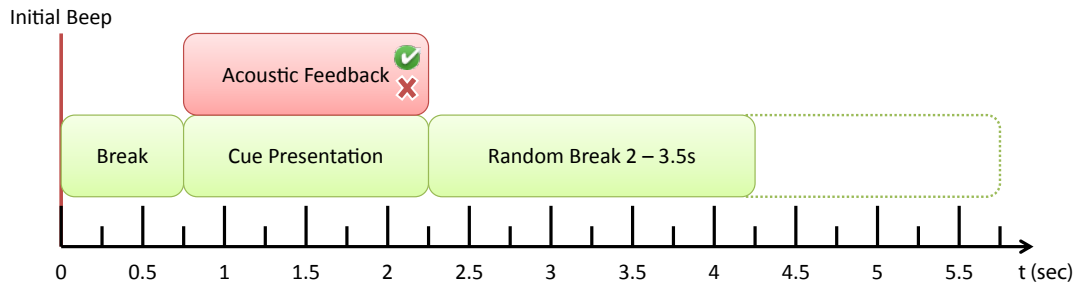

Figure 3.6: Illustration of a single trial of the paradigm used to control the test session. Each trial consists of an initial beep, a break of 750 ms, 1.5 s of cue presentation during which acoustic feedback is provided and a random pause of 2 s - 3,5 s.

3.5 Results

The section shows the results obtained during the experiment.

3.5.1 Performance of the Different Features

The CV accuracies of the best feature for each subject and the parameters C and γ for the SVM found with the grid search are given in Table 3.1.

Subject	Best Feature	$log_2(C)$	$log_2(\gamma)$	CV acc. (%)
S1	WL	5	-3	97.50
S2	WAMP	2	-1	99.64
S3	WAMP	5	-4	98.89
S4	WL	3	-3	95.89
S5	WAMP	7	-4	99.93
S6	WAMP	8	-6	96.36
S7	WAMP	2	1	96.00
S8	WAMP	2	0	97.50
S9	WAMP	7	-6	89.64
S10	HIST	4	-5	98.86

Table 3.1: Results of the training session. Best performing feature for each subject and the chosen parameters C and γ for the SVM.

An illustration of the performance of the different features is given in the box plot in Figure 3.7.

Table 3.2 shows the mean CV accuracies and the standard deviation for the different features.

The differences in the performances of the 10 different features for the 10 subjects have been tested by the means of an univariate ANOVA with a subsequent Newman-Keuls test to find out if the differences between the features were statistically significant. The result of the ANOVA was:

$$F_{(9,81)} = 68.85 \ , \ p << 0.01$$

The post hoc test showed that the performance of the features MDF and MNF is *significantly lower* than the performance of the other features. Also, the mean frequency feature (MNF) is significantly worse than the median frequency feature (MDF). Between the other 8 features no significant difference was found.
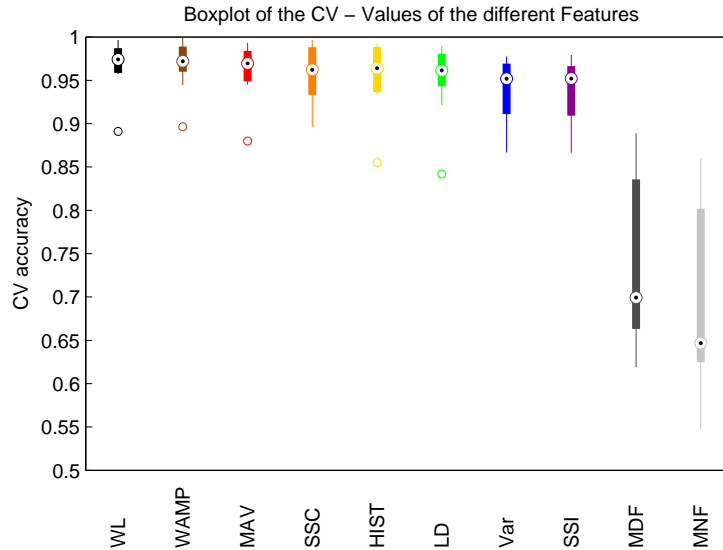
Figure 3.7: Box plot of the CV results of the ten different features for all subjects. The features are sorted from left to right according to their mean accuracies

3.5.2 Results of the Online Test

In this section the overall results of the online test are shown. Also, for some subjects a more detailed view on the individual results is provided.

The overall accuracies of the 10 subjects were in the range between 84.375% and 99.0625% with a mean of 92.75% and a median of 94.5313%. The individual results are given in Table 3.3.

Figure 3.8 illustrates the combined confusion matrix of all 10 subjects for the cue-based online test. The entries in the main diagonal are the class accuracies or the detection rate of the individual classes. An illustration of the class accuracies can also be found in Figure 3.9.

The differences in the class accuracies have been tested for their statistical relevance by the means of an univariate ANOVA. However, no statistical significance between the different classes has been found in terms of classification accuracy ($F_{(9,81)} = 1.73$, $p = 0.0964$).

The detection rate of the different classes has not been the same for each subject, however. In fact, some subjects had quite low accuracies for some classes. The resulting online accuracies per class for all subjects are given in Table 3.4. The corresponding confusion matrices for the individual subjects are shown in Figure 3.10.

Confusion Matrix (normalized) of detections within cue time for all 10 subjects
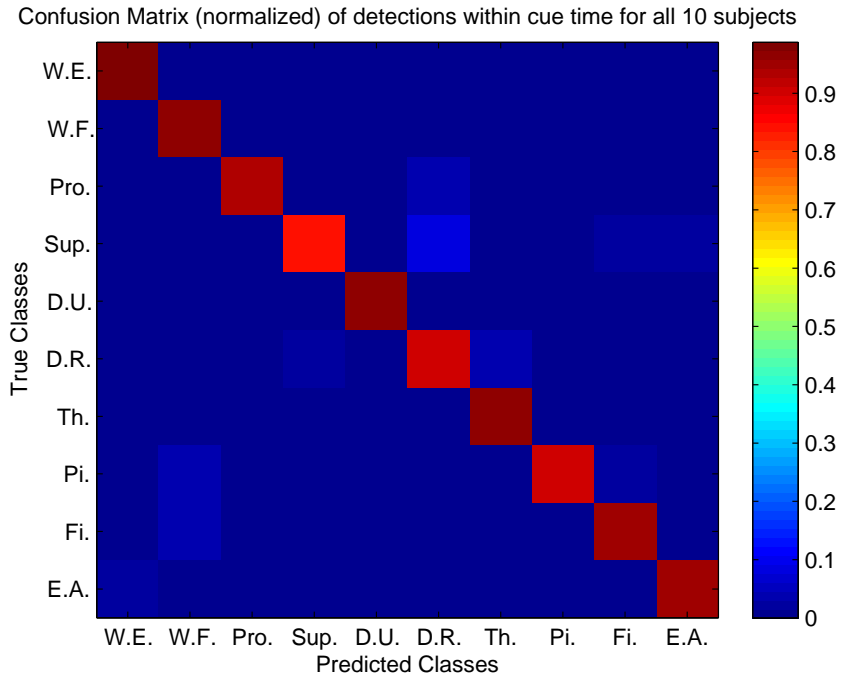
Figure 3.8: Combined confusion matrix for all 10 subjects over 3200 Trials. The best feature used for each individual subject and the respective SVM parameters are given in Table 3.1. The movements are labeled according to the abbreviations introduced in 3.4.1.
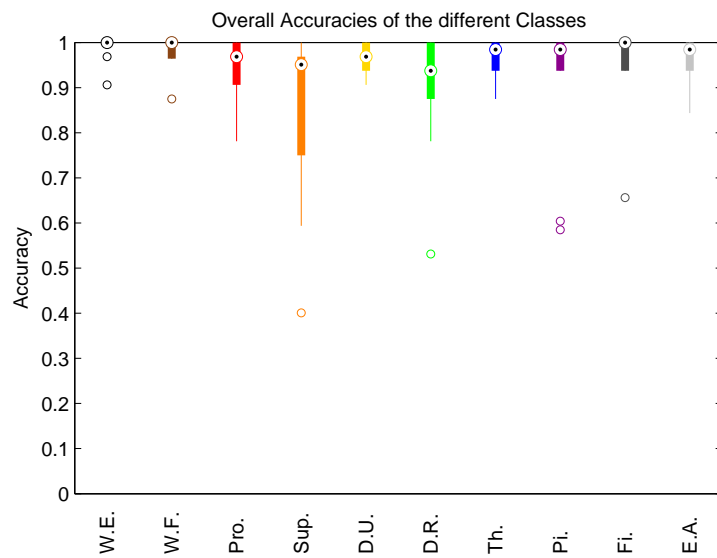
Figure 3.9: Resulting online accuracies for the individual classes.
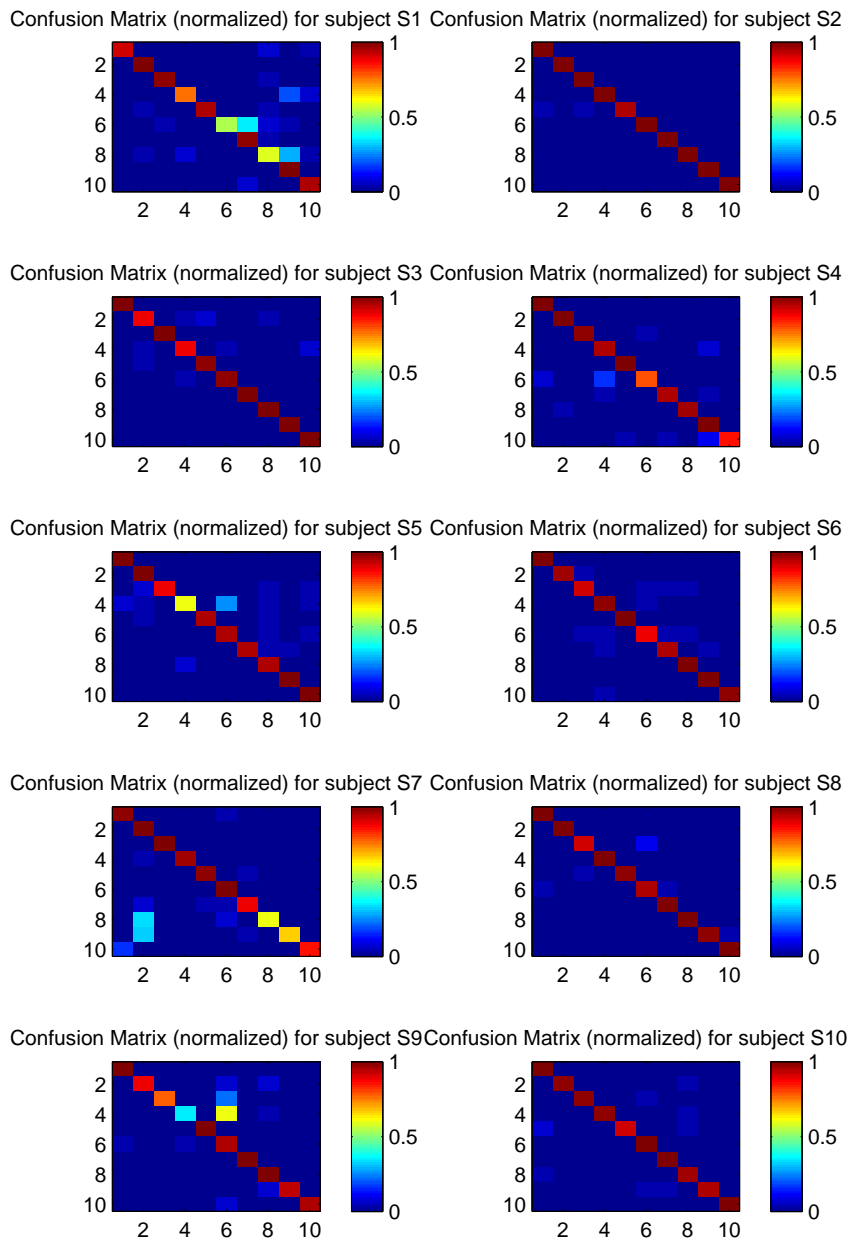
Figure 3.10: The individual confusion matrices for each of the ten subjects.

Feature	CV Result (%)
WL	96.74 ± 3.05
WAMP	96.72 ± 3.00
MAV	96.12 ± 3.33
SSC	95.91 ± 3.23
HIST	95.45 ± 4.16
LD	95.05 ± 4.33
Var	93.74 ± 3.74
SSI	93.70 ± 3.76
MDF	73.36 ± 9.76
MNF	68.07 ± 11.26

Table 3.2: Comparison of the CV results for the different features. All values are mean $\pm$ standard deviation. MDF and MNF features are significantly worse than the other features and MNF is significantly worse than MDF.

Subject	Result (%)
S1	85.625
S2	99.0625
S3	96.875
S4	93.125
S5	95.9375
S6	92.1875
S7	85.625
S8	97.8125
S9	96.875
S10	84.375

Table 3.3: Results of the cue-based online test.

Subject	W.E.	W.F.	Pro.	Sup.	D.U.	D.R.	Th.	Pi.	Fi.	E.A.
S1	0.9063	1	0.9688	0.7500	0.9375	0.5313	0.9688	0.5848	1	0.9375
S2	1	1	1	1	0.9375	1	1	1	1	1
S3	1	0.8750	1	0.8750	0.9688	0.9688	1	1	1	1
S4	1	1	0.9688	0.9375	1	0.7813	0.9375	0.9643	1	0.8438
S5	1	0.9643	0.9063	0.9688	1	0.8750	0.9375	1	1	0.9688
S6	1	1	0.8750	0.5938	0.9375	0.9375	0.9375	0.9375	1	1
S7	0.9688	1	1	0.9643	0.9688	1	0.8750	0.6042	0.6563	0.8438
S8	1	1	0.9063	1	0.9688	0.9375	1	1	0.9688	1
S9	1	0.9688	0.9688	0.9688	0.9063	1	1	0.9688	0.9375	1
S10	1	0.8750	0.7813	0.4009	1	0.9375	1	1	0.9375	0.9375
mean	0.9875	0.9683	0.9375	0.8459	0.9625	0.8969	0.9656	0.9060	0.9500	0.9531
± std	0.18	0.02	0.05	0.08	0.04	0.13	0.15	0.03	0.03	0.19

Table 3.4: Achieved online accuracies per class and overall for each subject.

Subject with the best performance

Subject S2 had the best online result, as can be seen in Table 3.3. The confusion matrix for this subject is illustrated in Figure 3.11. It can be seen that this result is very close to an ideal classification represented by the identity matrix. Only some instances of the "ulnar deviation"-class have been misclassified as pronation and wrist extension.
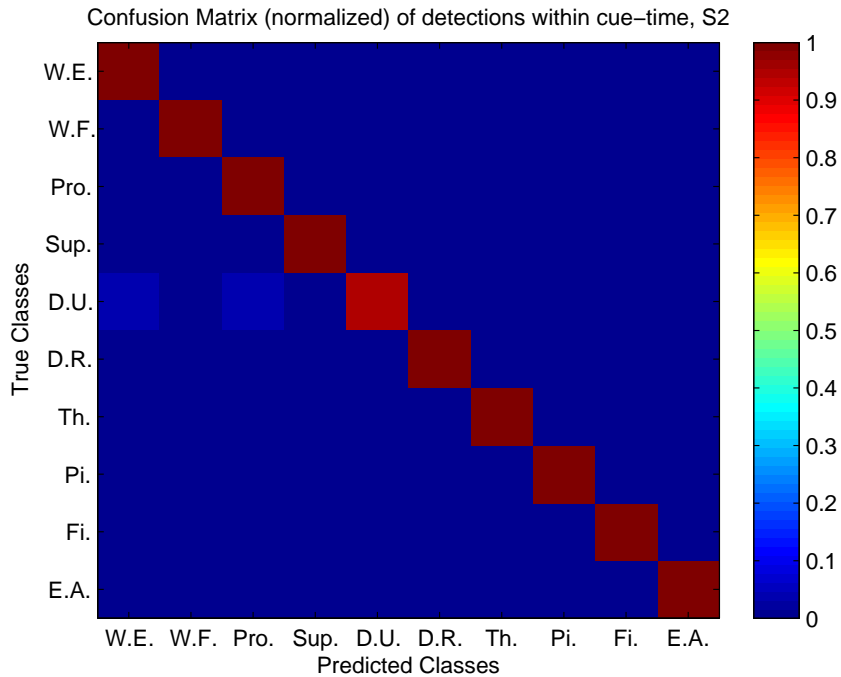
Figure 3.11: Confusion matrix of subject S2.

Subject with the worst performance

The lowest online accuracy was achieved for subject S10. Figure 3.12 shows the confusion matrix for this subject. It can be seen that especially the classes "pronation" and "supination" achieved low detection rates (78.13% and 40%, respectively). The confusion matrices of the four individual test runs of subject S10 are given in Figure 3.13. These images depict a degradation of the classification accuracy over time.

Subject S6 The results of subject S6 are also quite interesting. The overall online accuracy of S6 was in the middle range with 92.19% (see also Figure 3.14). However, looking at the detection rates of the individual test runs shows a high performance of 98.75% ind the beginning and a vast decrease of this performance over time (Figure 3.15)
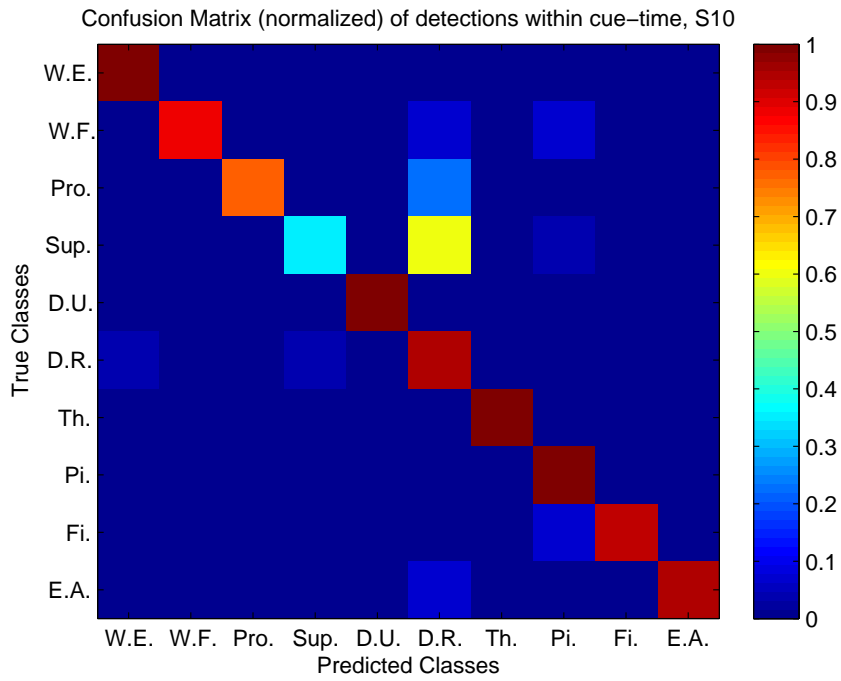
Figure 3.12: Confusion matrix of subject S10.
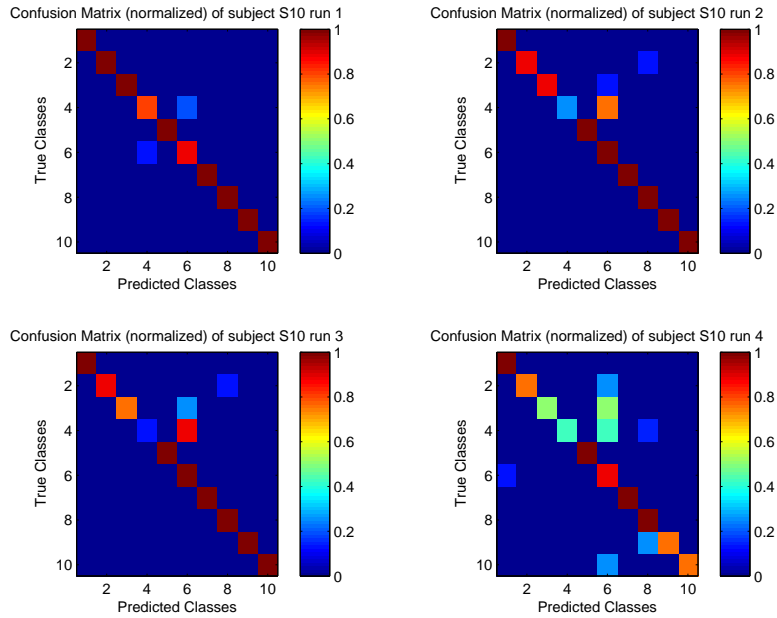
Figure 3.13: Confusion matrices of subject S10 for the four test runs.
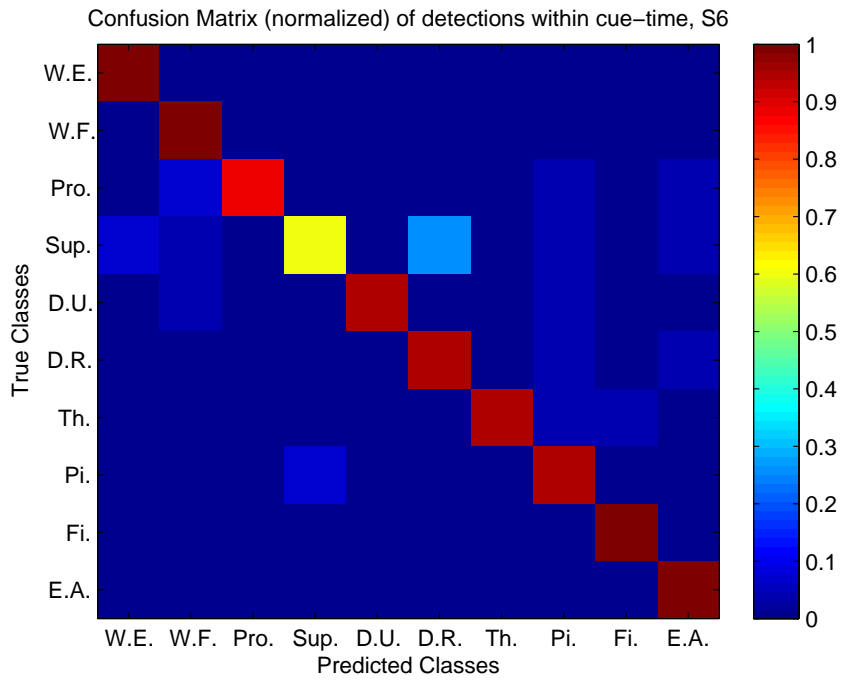
Figure 3.14: Confusion matrix of subject S6.
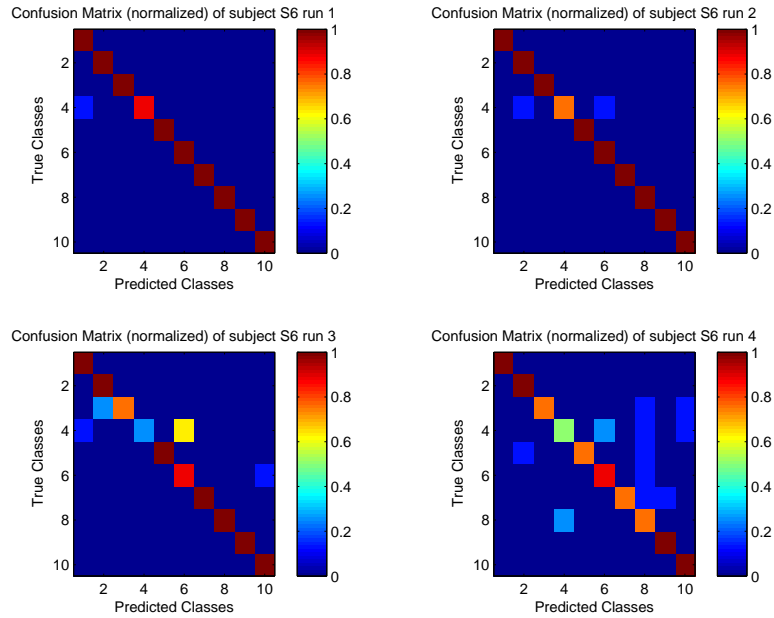
Figure 3.15: Confusion matrices of subject S6 for the four test runs.

3.5.3 Questionnaire Results

The results of the VAS on the questionnaires that were filled out by the subjects are provided in the following.

Table 3.5 shows the mean values and standard deviations for electrode disturbance and muscle fatigue throughout the experiments. The development of the investigated properties for each subject are shown in Figure 3.16.

Wearing Time	0 min	35 min	75 min
Electrode Disturbance	8.60 ± 1.68	9.14 ± 1.30	9.16 ± 1.16
Muscle Fatigue	8.51 ± 1.57	7.81 ± 2.03	7.18 ± 2.66

Table 3.5: Results from the VAS in the questionnaires for electrode disturbance and muscle fatigue. 10 always represents the highest score, 0 the lowest. In the case of electrode disturbance 10 means "not disturbing at all" and 0 means "extremely disturbing". In the case of muscle fatigue 10 means "not exhausted at all" and 0 means "extremely exhausted". All values are $mean \pm std$.
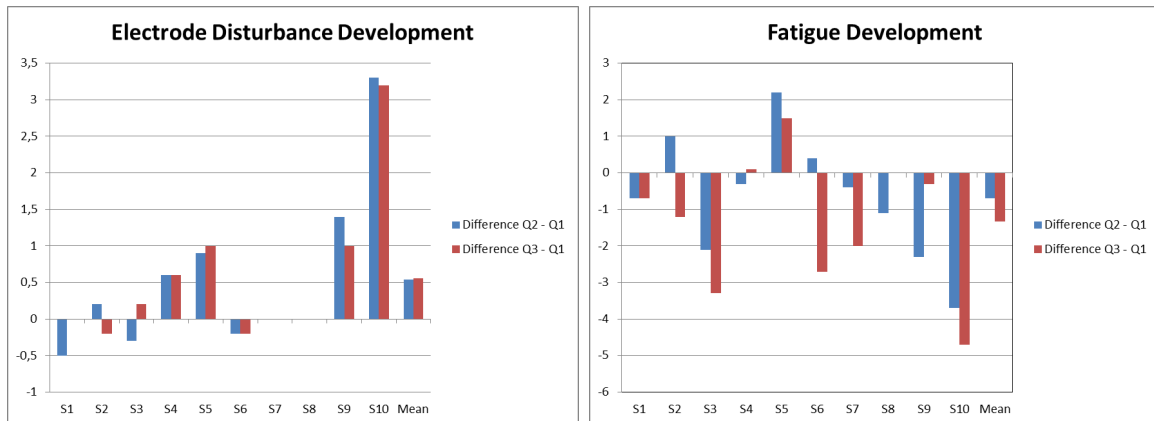
Figure 3.16: Development of the electrode disturbance- and fatigue scores from the VAS questionnaires. The blue bars represent the difference between the second and the first questionniare (after a wearing time of 35 minutes), the red bars show the difference between the third and the first questionnaire (after 75 minutes).

The differences of the values for electrode disturbance and muscle fatigue have been tested on their statistical relevance. The results are:

Fatigue $\qquad\qquad\qquad\qquad$ $F_{(2,18)} = 3.04$, $p = 0.0729$

Electrode Disturbance $\quad$ $F_{(2,18)} = 2.35$, $p = 0.1238$

Which means that the observed differences over time are *not* statistically significant.

3.6 Discussion of the Results

In this section the results of the experiments that were presented in the preceding section will be discussed thoroughly.

3.6.1 Performance of the Different Features

As already mentioned, the performance of the features MDF and MNF is *significantly lower* than the performance of the other features and the performance of the MNF feature is significantly worse than the MDF feature, while there is no statistically significant difference between the other features. The question arises why the only two features based on the spectrum of the EMG signal perform significantly worse than the time based features. Boostani and Moradi in 2003 [10] evaluated a variety of features with respect to their ability to separate 15 different classes (including the resting class) and their robustness against noise with data from 10 disabled people. In their comparison, the median frequency did not perform much worse than, for example, the waveform length feature. The sensitivity against noise, however, has been reported to be higher in this feature. So maybe the fact that, with regards on the user comfort and ease of use, no excessive skin preparation like dry shaving and abrasion has been performed led to increased noise in the EMG signal due to the higher electrode-skin impedance and hence led to the decreased performance. However, the results of this study can not be compared to the results of this thesis due to the fact that they used data from disabled people. But Oskoei and Hu [38] also investigated the performance decrease of different features when shortening the segment length of the data used for classification. They used data from 11 healthy subjects and found that the frequency domain features showed a decrease in classification performance when the segment length was shortened while the performance of the used time domain features was almost stable. The origin of their investigations was a segment length of 500 ms, so the segment length of 250 ms used in this thesis could be another reason for the lower performance of the two frequency domain features.

However, a longer segment length leads directly to a greater latency of the system and is thus undesirable. Another result is that, although no statistical significance is given, the mean accuracy of the waveform length feature was the highest, which is consistent with findings for single features in literature [38], closely followed by the Willison amplitude feature. This indicates that the usage of the waveform length feature would generally lead to good results when there is no time to perform a comparison of different features.

3.6.2 Results of the Online Test

Overall performance of the online system

The online system implemented in this thesis showed a good overall performance over 10 subjects and 3200 trials of 92.75%. However, the classification accuracy has not been the same for all different types of performed movements. Looking at the classification results per class given in 3.4, it seems that especially the supination, radial deviation and pinch classes performed worse than the others in general. Figure 3.10 shows that for four subjects at least one class had a quite low detection rate. In the case of supination, this could be caused by the fact that, like in [10] for example, no exclusive electrode has been assigned to the pronator teres muscle. But because the carpi radialis muscle is adjacent to this muscle, classification of this movement should still be possible. However, only a slight misplacement of the electrode could result in a relatively large decrease of detected activation from the pronator muscle. The radial deviation class has mostly been confused with an extension of the thumb or supination. When performing a radial deviation it is, however, quite common among all subjects to extend the thumb during the movement. The subjects stated that this would be the natural way of them performing this movement. The confusion with supination probably occurred due to a slightly pronated resting postition. Since only the 250 ms of the signal are extracted for classification this could easily result in such a misclassification. The pinch class has quite often been confused with the class for making a fist. These movements however have relatively similar patterns, at least with regard to the muscles the signals are derived from. A very strong pinch grasp is therefore quite likely to be confused with a fist. The confusion of both the pinch and the fist movement with wrist flexion most likely results from the observed tendency of the subjects to slightly flex their wrist during these motions. Generally, some subjects stated that the individual movements did not seem totally natural to them and that in normal everyday situations they performed combinations of the movements more often.

Subject S2

Subject S2 showed an almost perfect performance during the online test. Only 3 out of 320 movements have been classified incorrectly and one of the was because the subject missed the cue due to a lack of focus at this moment.

Subject S10

As mentioned before, the online system showed the worst performance for subject S10. Especially the classes pronation and supination achieved low accuracies of 78.13% and only 40% respectively. This means that the supination class did hardly work with this subject. In fact, subject S10 stated that performing this movement was exhausting and, with an increasing number over time, even failed to exceed the threshold for onset detection in some of the trials. Also, according to the VAS results from the questionnaires, subject S10 stated to be most exhausted among all subjects (see Figure 3.16). Of course, a dispositioning of the electrodes is another possible explanation for the shown results. Especially since the supinator muscle is in the deep layer of the posterior compartment and a bipolar derivation has been used, a suboptimal electrode position could result in a greatly attenuated signal from this muscle. Unfortunately, there is no perfect solution to the problem of electrode dispositioning since the location of the individual muscles varies slightly for each subject.

Subject S6

Subject S6 (left handed) showed vastly decreasing performance over the 4 testing trials. When using the non-dominant hand for EMG measurements several factors have to be taken into account. A number of researches have addressed the influence of hand dominance on muscle fatigue, motor unit firing behavior, differences in the EMG signals and differences in movement coordination [3; 5; 18; 22; 46]. It has been found that the EMG activity varies between the same movements performed with the dominant and the non-dominant side [18]. However, this should not have an influence on the performance of the system since the classifier is trained based on the underlying EMG signals and the CV-accuracy has been quite high. But it has also been found that hand dominance has an impact on the manifestation of muscle fatigue in the upper trapezius muscle. It has been shown that the non-dominant side has a statistically significant higher fatigability in both the right- and the left handed subject group [22]. Although this investigation has been performed on a different muscle group it seems reasonable that the non-dominant arm would show larger liability for fatigue to occur since the dominant side is usually

better trained because of preferred use in daily activities. However, this is a real issue, since a system for the application in the control of an active prosthesis should work for both the dominant and the non-dominant hand for obvious reasons.

Another issue could be overfitting. Looking at Table 3.1, the parameter C (i.e. the slack variable) that was used to train the classifier for subject S6 shows a high value of $2^8 = 256$. As mentioned in 2.2.1, C controls the upper boundary of the VC-dimension and hence a large value for C indicates a tendency towards overfitting which leads to a bad generalization of the trained classifier. Such an overfitting classifier would be very sensitive to changes of the features used as input data. This could explain the vast decrease in classification performance observed in subject S6. The features could have undergone small changes over time due to increasing muscle fatigue, maybe worsened because of the fact that the non-dominant hand was used for the experiment, which would lead to the observed behavior when a classifier with bad generalization is used.

3.6.3 Questionnaire Results

The questionnaire assessed the questions whether the subjects were bothered by the electrodes or if the movements that have to be performed to control the system caused uncomfortable exhaustion in the muscles of the forearm. The discomfort caused by the electrodes mounted to the skin generally did not seem to be unreasonably high. It is however quite interesting that most of the subjects felt less disturbed by the electrodes at the end of the measurement than at the beginning. However, across all subjects this decrease in the disturbance level has not been statistically significant. The exhaustion of the muscle on the other hand could, at least in some subjects, represent a major limitation of the system. This fact would become even more critical for users that do not have a fully functional muscular structure in the forearm (e.g. transradial amputees or post-stroke patients). But also for this value, even though some subjects stated that they felt an exhaustion of their muscles, the differences over time have not been statistically significant. But this only means that exhaustion does not seem to be a general problem and for individual subjects it could still represent a limitation of the system.

4 EMG Game Control

The intention of this thesis was to implement a system that can be used for the control of an active prosthesis. However, such a device has not been available in order to test the real life performance of the algorithm. Instead it has been decided to use the system as an input device for Human-Computer Interaction (HCI). This area is also an important possible application for a control system based on sEMG signals. For example, using a system based on the EMG signal of facial muscles, like presented in [39], could provide easier access to computers for persons with paralyzing medical conditions. In the area of rehabilitation (e.g. post-stroke rehabilitation), an EMG HCI could be used to motivate patients to exercise by assigning them an entertaining task [50]. For healthy users, EMG based HCI could offer new and enhanced experience in computer games. For example, natural movements of the human arm could be mapped to different control signals for the computer in order to make the interaction with the computer more intuitive. This application for computer games is what has been implemented for this thesis. Research in this area has also been conducted by Microsoft[TM] [29] who have also been granted a patent for a wearable EMG device that can be used to acquire input signals for games. The experiment that has been conducted will be explained in the following section.

4.1 System Setup

The signal recording hardware used for this experiment as well as the respective settings have been the same as in 3. However, in this experiment two separate computers have been used - one for signal acquisition and classification and the other one for translating the classifier commands into game commands via the Graz BCI Game Controller developed by Markus Pröll [43], presenting visual feedback as an overlay on the game screen and running the gaming application (Figure 4.1). The communication between those two machines has been realized via TCP/IP. The signal processing on machine A has again been accomplished in Matlab and Simulink.

4.2 Gaming Application

The computer game Portal 2 (© 2011 Valve Corporation) has been chosen for the gaming application. Portal 2 is a first person puzzle platform game in which the user has to control an avatar in a 3D environment and solve different puzzles without a time constraint. To do this, the player can use a device to shoot two different portals (orange
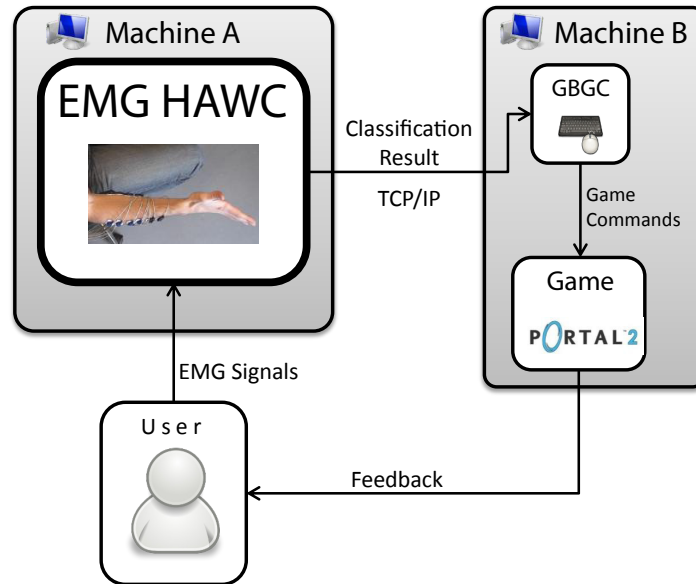
Figure 4.1: Illustration of the game control system consisting of two separate computers. The first machine runs the EMG **H**and **A**nd **W**rist movement **C**lassifier (HAWC), while the second machine interpretes the commands that are sent from the Classifier via TCP/IP and translates them into game commands to control the avatar. The gaming application itself represents the feedback to the user.

and blue) that are capable of transferring any object bidirectionally from source to destination. The player can also use a cube as an auxiliary device to solve some of the tasks. The cube can be used to deflect a laser beam or to trigger switches by its weight. Figure 4.2 (a-c) shows the usage of the cube for laser beam deflection and how portals can be used to pass the laser beam from source to destination. In Figure 4.2 (d-f) the cube is used to trigger a switch by its weight.

In order to control the game with the results of the sEMG classification system, the most important commands of the game had to be mapped to the different movements the system is able to distinguish. This command mapping can be found in Table 4.1. For the action controls a dwell timer of 1s has been introduced in order to minimize false activations. This is important since an unwanted activation of one of these commands can have a large negative impact on the level progress.
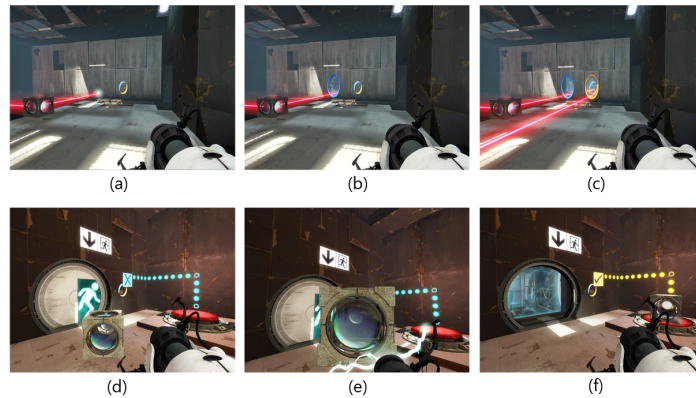
Figure 4.2: Usage of portals and the cube in Portal 2. The cube can be used to redirect laser beams (a) or to trigger switches (d-f). The two portals transport any object from source to destination (b,c).

Game Action	Mapped Movement
Action Controls	
Blue Portal	Pronation (Pro.)
Activate	Pinch Grasp (Pi.)
Orange Portal	Supination (Sup.)
Movement Controls	
Walk Forward	Fist (Fi.)
Walk Backwards	All fingers extension (E.A.)
Turn Left	Wrist flexion (W.F.)
Turn Right	Wrist extension (W.E.)
Look Up	Radial Deviation (D.R.)
Look Down	Ulnar deviation (D.U.)
Jump Forward	Thumb extension(Th.)

Table 4.1: Mapping of hBCI signals to the game commands.

4.3 Experimental Procedure

This section describes the experiment conducted to test the performance of the system in a self-paced online scenario controlling a gaming application. The movements that had to be classified and the placement of the electrodes has been the same as in 3.4.1 and 3.4.2, respectively, and will hence not be covered again here.

4.3.1 Subjects

This experiment has been conducted with two subjects. Both of the subjects were male and right-handed. The age of the subjects was 26 years and 27 years, respectively. Both of the subjects already had experience with first person games.

4.3.2 Phases of the Experiment

The experiment in total consisted of four different phases (Figure 4.3). A preparation phase where the electrodes have been applied and the subjects have been informed about the experiment, a training session, a cue-based testing session to get an objective measure of the classifiers performance and the self-paced gaming application.
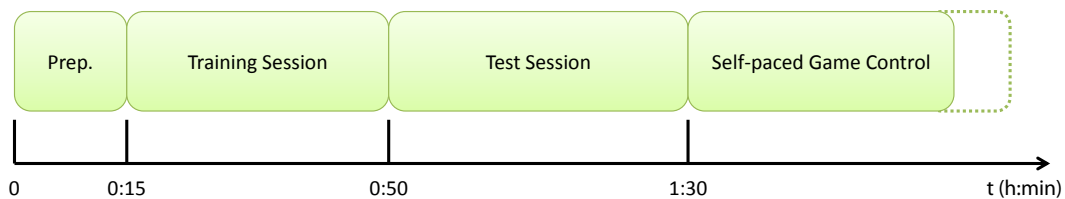
Figure 4.3: The different phases of the game control experiment. The first step is a preparation phase, where the electrodes are applied, followed by a training session, a cue-based test session and finally the self-paced gaming application.

The first three phases have been conducted in the same manner as in 3.4.4 and hence will not be described again in this section. Also, like in 3, the best performing feature for each subject has been calculated for 250 ms of data and used for the online test.

Game Control Session

The game control session started with an introduction of the subject to the game in general and the two levels (Level 2.1 and 2.2) that had to be completed during the test. After this introduction the subject first completed the level using the mouse only as a reference. To eliminate the experience of the subjects with computer games to some degree, all of the essential control signals have been mapped to the different buttons of

the mouse instead of using both mouse and keyboard. After this, the sEMG classification system has been used as the only control input to complete the same two levels. In this scenario the system worked in a self-paced manner, so no cues have been presented. The subjects navigated freely in the levels trying to solve the necessary tasks.

4.4 Results

The results of the training session, the cue-based online test and the game control session are presented in this section.

4.4.1 Results of the Training Session

After the training session the classifier has been trained with the best performing feature for each of the subjects based on the CV results, like in the feature comparison study, to find out if the best performing features of this study would also be chosen in this scenario. The cross validation results and the chosen feature with the respective parameters are presented in Table 4.2.

Subject	Best Feature	$log_2(C)$	$log_2(\gamma)$	CV acc. (%)
SP1	WAMP	6	-4	99.89
SP2	WAMP	4	0	96.71

Table 4.2: Results of the training session including the best performing feature for each subject and the chosen parameters C and γ for the SVM.

4.4.2 Results of the Cue-based Online Test

Also in this experiment a cue-based online test has been performed. This has been done in order to have some sort of objective measure for the performance of the classifier used in the self-paced scenario. The result of this test are the two confusion matrices in Figure 4.4. The achieved accuracies for the two subjects have been 95.94% and 97.81%, respectively.

4.4.3 Results of the Game Control Session

In the game control session the in-game commands had to be addressed via the different hand movements. Two examples of this are shown in Figure 4.5 and Figure 4.6, respectively.
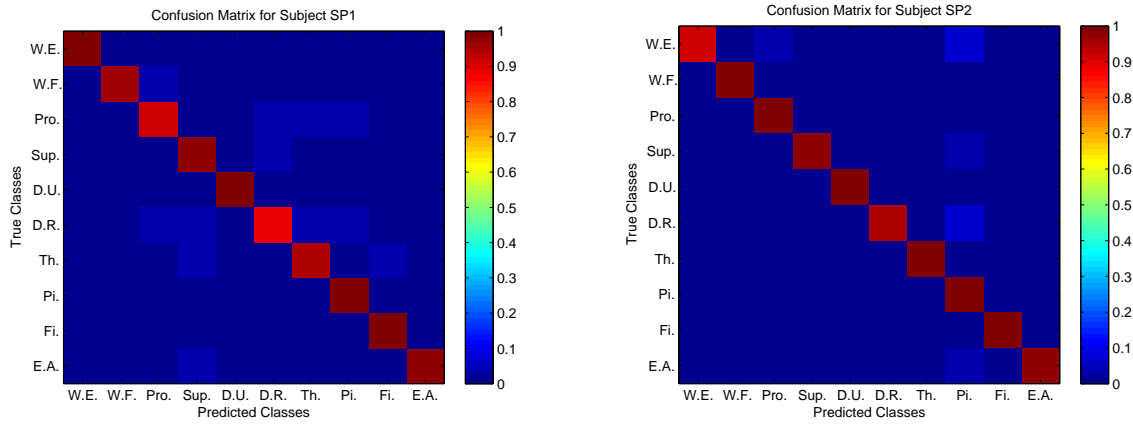
Figure 4.4: Confusion matrices of SP1 and SP2 for the cue-based online test that has been conducted prior to the gaming application.

Both of the subjects completed the two levels using the EMG control system. The time taken to complete the levels is given in Table 4.3.

Level	Input modality	SP1	SP2
2.1	Mouse	0:36	0:39
	EMG	1:48	1:15
2.2	Mouse	1:24	1:13
	EMG	7:16	4:45

Table 4.3: Comparison of level completion times using the mouse and the sEMG classification system as input modalities.
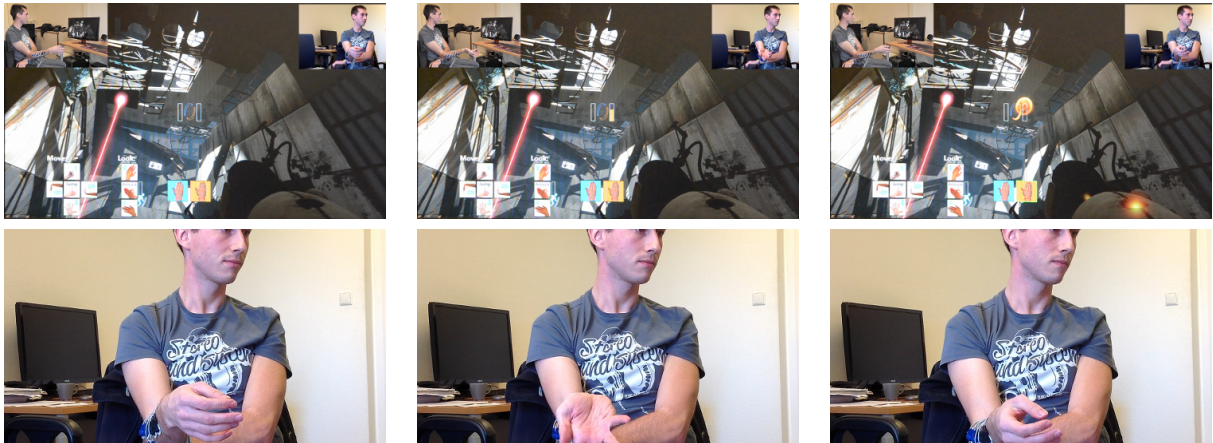
Figure 4.5: Shooting an orange Portal in Portal2. The images are sorted from left to right, the images in the upper row show the in-game screen and the users actions while lower row show the actions of the user, only zoomed. On the left hand side the user has already aimed at the right position and is now ready to initiate the portal action. In the middle the user performs a supination which causes the dwell timer to start rising. On the right hand side the dwell timer has reached its maximum and the portal has been fired. The user has returned to his resting position.
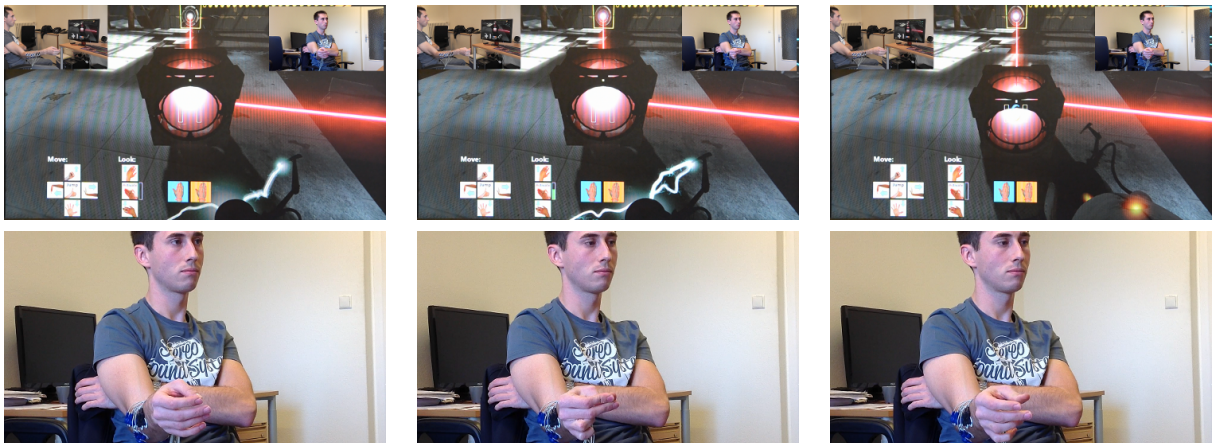
Figure 4.6: Dropping the cube in Portal2. Again, the images are sorted from left to right. The left hand side shows the starting position of the cube drop action where the user has already aimed in the right direction. The images in the middle show the user performing a pinch grasp, the dwell timer for the "activate" command starts rising. On the right hand side the dwell timer has reached its maximum and the action was triggered resulting in a cube drop.

4.5 Discussion of the Results

4.5.1 Results of the Training Session

From Table 4.2 it can be seen that for both of the subjects the best performing feature was WAMP. This feature has already been chosen for the majority of subjects in the feature comparison study. This suggests that this feature is generally well suited for distinguishing between the different movements in this setup. The cross validation accuracy has been quite high for both subjects with moderate choices for the SVM parameters.

4.5.2 Results of the Cue-based Online Test

The results of the cue-based online test have been quite high for both subjects. Looking at the confusion matrix for subject SP1 (Figure 4.4 shows that the system had some problems with classifying the pronation and the radial deviation classes. The performance for subject SP2 has been a bit higher, but the confusion matrix indicates a bias of the classifier towards the pinch grasp class, since nearly all of the misclassified movements have been classified with this label. This issue could be addressed by using different electrode positions or different movements for classification in the future.

4.5.3 Results of the Game Control Session

Both subjects were able to complete the levels without any assistance. However, subject SP1 had a relatively high completion time for level 2.2 of over 7 minutes. One problem for S1 was that during the gaming session it was suddenly very difficult to achieve a sustained activation for some classes. The problem was that between the cue-based test and the gaming session the subject and the recording hardware had to be repositioned. This was necessary because the cues have been presented on the machine that was doing the classification and the gaming application was running on the other machine. During this repositioning tensile loading of the electrodes occurred which may be one explanation for this behavior. Due to this issue, the perceived level of control for SP1 has been quite low. For subject SP2 this repositioning has been avoided by putting the screens of the two computers next to each other. Because of this the gaming application could be controlled from the same position as the cue-based test. Subject SP2 reported no issues regarding the sustained activation of commands and the perceived level of control was high. The tensile loading for subject SP1 is also partly caused by the bulky measurement setup that would have to be changed for future applications.

5 Hybrid System

In addition to the previous experiments the sEMG classification system, this time only distinguishing between 7 classes, has been combined with a with a three-class Steady-State Visual Evoked Potential (SSVEP) Brain-Computer Interface (BCI) in order to form a hybrid BCI (hBCI). A BCI is a system that is able to derive control signals from the users electroencephalogram (EEG) SSVEPs are responses of the human brain in the visual cortex that occur when the user focuses on flickering lights and can be measured in the EEG [56]. Hybrid BCIs are combinations of a BCI and and another system that can be another BCI ore some other system [40]. The use of a hybrid system only makes sense if the combined system achieves specific goals better than the conventional BCI. In the case of a SSVEP BCI in combination with an sEMG classification system the benefit would be a higher Information Transfer Rate (ITR) and a lower latency. A comparison of the ITRs and latencies of different BCI paradigms and a system based on EMG can be found in Table 5.1. For more information on BCIs and the different Paradigms the reader is pointed to [47; 58].

Paradigm	ITR (bits/min)	Latency (sec)
LRP	20	-0.120
P300	28.2	1.58
ERD/ERS	28.8	1.5
SSVEP	26.4	2.10
Sensorimotor cortex rythms	16.8	2.20
SCP	3.6	65.75
EMG	99.6	0.96

Table 5.1: Comparison of the ITR and the latency of different BCI Paradigms and EMG [42].

5.1 Signal Recording Hardware

For this experiment again two computers have been used that communicated via TCP/IP. One machine was again responsible for the acquisition of the sEMG and EEG signals and subsequent classification while the other machine was presenting the SSVEP stimuli and feedback, translating the commands and running the game application (Figure 5.1). The biosignals were recorded using two g.USBamps. The amplifier for the sEMG again recorded with a sampling frequency of 2400 Hz and a band pass filter from 5 Hz to 500 Hz as well as a notch filter were applied. The EEG (13 channels over the occipital cortex, Figure 5.2) was recorded using a sampling frequency of 1200 Hz, a 0.5 Hz to 100 Hz bandpass filter and notch filtering.
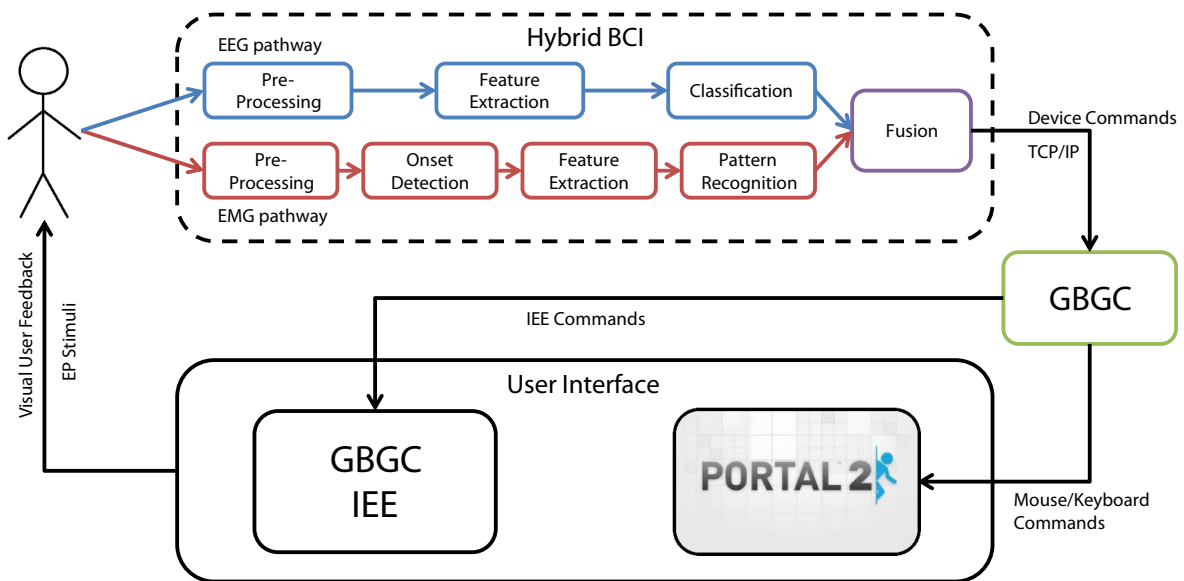
Figure 5.1: The hybrid system consisting of a three class SSVEP BCI combined with the seven class on-line EMG classification system. The classification results of the two systems are transmitted to the second computer via TCP/IP. The second machine translates these commands into mouse and keyboard inputs to move the avatar and controls the interface extension engine (IEE) that provides feedback for the user.
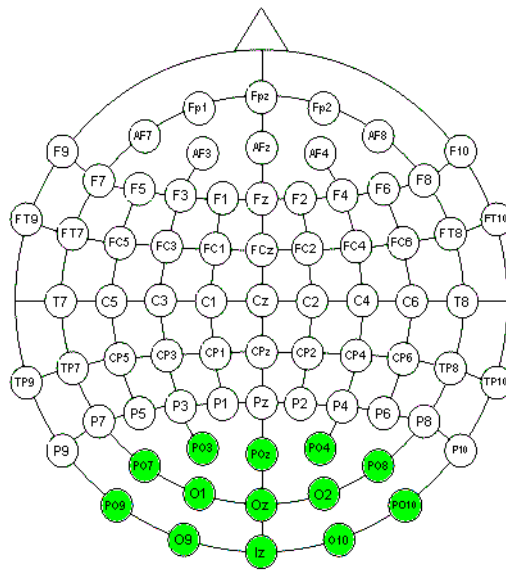
Figure 5.2: Electrode positions according to the 10/20 system. The 13 used occpital electrodes are marked in green.

5.2 Biosignal Classification

The classification algorithm for the frequency-coded SSVEP system has been provided by Tobias Oesterlein [37]. This system is based on Canonical Correlation Analysis (CCA) [27; 31] in combination with a Linear Discriminant Analysis.

For the 7-class sEMG classification system the same onset detection and classification algorithms as in the previous experiments has been used. However, instead of using a single feature a combined feature vector consisting of three features has been used. These three features have been WL, WAMP and MAV, since in 3.5.1 these features had the highest mean values when comparing the CV results of all 10 feature extraction method applied to the data of 10 subjects (Figure 3.7, Table 3.2). The intention was that a combination of three features would lead to a more powerful feature vector and hence a better overall performance.

5.3 Gaming Application

The gaming application for this experiment was the same as in 4.1. The 10 in-game commands have been divided into two sets of 3 and 7 commands, to be addressed by the two classification systems. The action commands in Table 4.1 have hereby been controlled by the SSVEP system, the movement controls have been addressed by the sEMG system. The respective hand movements for the 7 movement controls have been the same as in the EMG game control experiment.

5.4 Experimental Procedure

As already mentioned the movements to address the 7 EMG-controlled in-game commands were the same as in the previous experiment, only excluding pronation, supination and pinch grasp. Since the movements have been mostly identical also the same electrode position have been chosen for signal acquisition.

5.4.1 Subjects

The experiment has been conducted with two subjects that have already participated in the previous experiments (i.e. S1 and SP2). Both of these subjects are right-handed and already had experience with the game Portal 2.

5.4.2 Phases of the Experiment

The procedure of the experiment is illustrated in Figure 5.3. First the preparation for the EMG recording and the EMG training session consisting of two runs of 70 trials each have been conducted. The training paradigm was the same as for the previous experiments, but only showing 7 cue images of course. After that the EEG electrodes have been applied and a screening session has been conducted in order to find the three best suitable stimulation frequencies in the range of 9-30 Hz. Then the subjects had to complete the two levels in the game. Finally the performance of the EMG classifier has been assessed by a cue-based online test. This test consisted of three runs with 70 trials each.
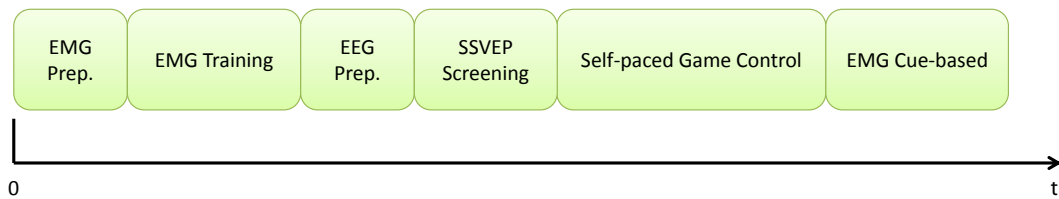
Figure 5.3: The different phases of the hybrid experiment. First the preparation for the EMG recording and the EMG training has been conducted, followed by the preparation for the EEG recording and the SSVEP screening and the game control. After this, the performance of the EMG classifier has been assessed by a cue-based test.

5.5 Results

In this section the results of the EMG part of the hybrid system are presented.

5.5.1 Results of the Training Session

The CV results on the training set and the parameters for the SVM found via grid search are given in Table 5.2.

Subject	$log_2(C)$	$log_2(\gamma)$	CV acc. (%)
S1	0	-4	96.86
SP2	0	-3	99.29

Table 5.2: Results of the training session in the hybrid experiment including the chosen parameters C and γ for the SVM.

5.5.2 Results of the Cue-based Online Test

Again a cue-based test has been performed to assess the performance of the EMG classifier. The classification accuracies have been 97.14% for S1 and 99.52% for SP2 on the data set of 210 trials. The confusion matrices are illustrated in Figure 5.4.
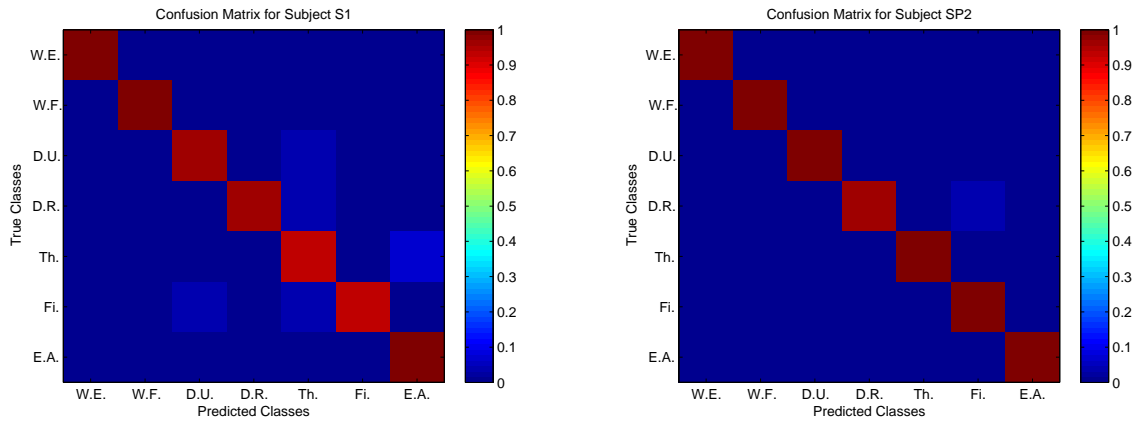
Figure 5.4: Confusion matrices of S1 and SP2 for the cue-based online test that has been conducted in the hybrid experiment.

In this experiment also the issue of erroneously detected onsets when no action was intended by the user was investigated. For this purpose the inter-trial periods have been investigated. In these periods a total number of 34 false onsets has been detected for both subjects with a mean length of 75.4 ms. The effect that the application of a dwell timer would have on the number of erroneous onsets is shown in Figure 5.5.
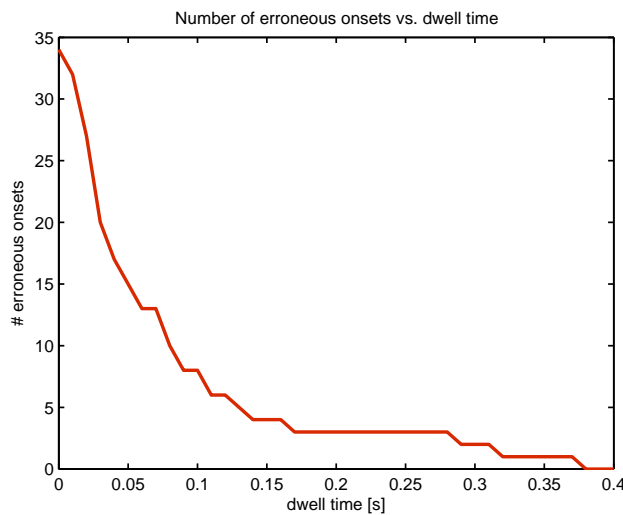
Figure 5.5: Illustration of the influence of a dwell timer on the number of false activations.

5.5.3 Results of the Game Control Session

In the game control session the completion time for the two levels have again been compared for the two different input modalities (i.e. hBCI and mouse). The results can be found in Table 5.3.

Level	Input modality	S1	SP2
2.1	Mouse	0:33	0:32
	hBCI	1:56	1:15
2.2	Mouse	1:06	0:54
	hBCI	3:30	4:40

Table 5.3: Completion times for the 2 played levels in Portal 2 using the hBCI system and the mouse as a reference input modality.

5.6 Discussion of the Results

5.6.1 Results of the Training Session

Both subjects achieved high CV accuracies based on the training data. The chosen values for the parameter C suggest that the tendency of the classifier to overfit could be less distinct than in 3. This could be caused by the fact that a combined feature vector has been used for this experiment, but also by the fact that this was only a 7-class problem. Another factor is that the subject already had experience with the experiment and hence maybe performed better during the training phase, for instance by performing the movements more consistently.

5.6.2 Results of the Cue-based Online Test

Both subjects showed a very good performance of 97.14% and 99.52%, respectively. For subject SP2 only one class (ulnar deviation) had a detection rate below 1. For subject S1 misclassifications occurred in four of the classes, many of which were classified as an extension of the thumb. This indicates a bias of the classifier towards this class. The investigation of the effect that a dwell timer would have on the number of erroneous onsets showed that the introduction of a dwell timer of only 50 ms would lead to a decrease of erroneous onset detections from 34 to 15 without a decrease of true positive onsets and the latency of the whole classification system would still be within the 300 ms range.

5.6.3 Results of the Game Control Session

The time to finish the individual levels with the hBCI systems has been $2 - 4$ times as large as the completion time with casual input devices for both subjects. This difference can not be explained with the latency of the system only. Especially because once a movement, e.g. walk forward, is detected the user usually keeps up the action for several seconds so that the influence of the latency is smaller. However, aiming in a 3D environment using the EMG signals is not as precise as aiming with a mouse since there is a latency between the users return to the resting position and the recognition of this resting position by the onset detection unit. Hence the mouse speed had to be lowered in order to accomplish the necessary aiming tasks.

6 Discussion and Conclusion

6.1 General Aspects

Measurement Setup

The implemented system consisted of a (stationary) measurement PC, a biosignal amplifier and 17 electrode cables and electrodes that have been attached to the users forearm. This setup is pretty much fixed to a single location and limits the users movement range. Additionally, the 17 single electrode cables had to be formed into a strand of cables and attached to the users arm for artifact prevention. For a practical use of the presented system on a regular base some adaptations would be desirable. For instance, the measurement hardware would have to become smaller and, ideally, attached to the user (e.g. his arm) to guarantee mobility. Also the 17 electrode cables seemed quite bulky, so either a reduction of necessary electrodes or a more sophisticated setup would be advantageous. Also, using dry electrodes that are integrated in some sort of sleeve that can simply be pulled over the forearm, like in [57], seems very advantageous.

Electrodes

The electrodes used for this work were monopolar electrodes. Bipolar electrodes, ideally with only a single connection cable would be of great advantage since this would reduce the application time and the number of electrode cables. It has also been observed that for subjects with hairy forearm, the adhesion of the electrodes decreased over time and the electrodes tended to lose contact to the skin. This could be overcome by using some sort of sleeve with dry electrodes in it instead of adhesive electrodes.

Cue Presentation

Even though it was attempted to present cue images that present the required movements in a comprehensible way, some of the subjects expressed that they had problems distinguishing some of the cues, at least in the relatively short time they were presented. Maybe an animation showing the movement itself and not just the final position would be more suitable for the task and would prevent possible wrong movements. Especially in the training phase a minimization of wrong movements would be desirable since otherwise the training data is contradictory.

SVM Training Time

One problem concerning the cue-based online test was related to the training time of the SVM. Because of the fact that 10 different features have been evaluated, the grid search for the parameters C and γ for the SVM had to be conducted for each of the possible features. If combined feature vectors of multiple features are to be evaluated this problem becomes even bigger, because the number of possible combinations depends on the number of available features and the number of features chosen to combine into one vector.

If there are n different features, and every combination of k of those features should be tested, the number of possible combinations is determined by:

$$\frac{n!}{k!(n-k)!}$$

It can be seen easily that this number tends to get quite big really fast, for instance for all possible combinations of up to two Features already 55 grid searches for the best parameters would have to be conducted. The big problem with this is that the comparison of the different feature combinations has to be done between training and online test, while the subjects are still connected to the measurement hardware. So it is clear that this time has to be kept as short as possible. Unfortunately, even though the source code of LIBSVM has been optimized to operate on all four processors of the computer used in this work, the calculations to find the best single feature for the subject (i.e. 10 grid searches with CV) already took six minutes. For future work, the best single feature of the feature comparison study or a combination of the best features could be used to avoid this long training time.

Experiment time

Another issue regarding the training is the time it takes to record all the necessary data. Each training run consisted of 70 Trials (i.e. 7 per class) and a took about six minutes to finish. Four of these runs have been conducted to get 28 training samples per class in order to limit the possibility of overfitting. However, looking at the parameters that were chosen during the grid search in Table 3.1 and keeping in mind that a large value for C leads to overfitting on the training data (as described in 2.2.1) it can be seen that there is potential overfitting for some subjects. This could mean that there are still too few training samples to train a robust classifier. On the other hand, recording more data means elongated training sessions, and some of the subjects mentioned that the training is kind of repetitive. Most of the subjects said that the feedback run,

although the only difference was the acoustic feedback if a movement was correctly classified, was much more interesting. Maybe this could be used to ones advantage if the classifier is first only trained with a few samples per class and the data from each of the online runs is then added to the training set. Of course one could implement some kind of more sophisticated feedback like a simple game which would probably result in a higher subject motivation. Applying these changes to the training phase that has to be conducted before an application can be controlled would result in a subject with higher motivation and a more robust classifier.

Another option could be to restrict the parameter C to lower values, which could result in lower CV results but a better generalization. Also, instead of the C-SVM used in this thesis, a ν-SVM could be used. In this variant of the SVM the parameter ν is in the range between 0 and 1 and indicates the fraction of training samples that are used as support vectors and hence allows better control of the number of support vectors used.

Erroneous Onset detections

For an online control application a good classification accuracy alone is not enough. While playing Portal 2 it became obvious that erroneous detections of a movement onset have a negative impact on the gaming experience since in the worst case they could lead to a situation where all the work that has been done so far in the level is annihilated. It has been shown that the introduction of a dwell timer could significantly reduce the number of erroneous onsets. But of course there will always be a trade-off between these erroneous detections and the latency of the control system.

6.2 Conclusion and Future Perspectives

The system presented in this thesis is capable of distinguishing between 10 different gestures with a high overall performance. Based on the results of the feature comparison experiment, a combined feature vector that promises good general performance has been found and it has been shown that the system can operate in a self-paced manner. The experiments in this thesis have been conducted with healthy subjects, however, Tenore et. al in 2009 [53] have compared the accuracies of able-bodied subjects with those of a transradial amputee and there was no significant difference. This means that the system presented in this thesis would also be applicable for transradial amputees and could thus be used to control actice hand prostheses. But of course there is room for improvement in the future. For example a more mobile setup would be desirable, maybe using an electrode sleeve and some embedded system for signal processing. Also the application of a regression algorithm could be beneficial for the control of active prosthesis and thus would be worth investigating in the future.

References

[1] `http://bio-medical.com/media/support/H124SG.pdf` (accessed April 2012).

[2] `http://www.shadowrobot.com/hand/competitors.shtml` (accessed April, 2012).

[3] Alexander Adam, Carlo J. De Luca, and Zeynep Erim. Hand Dominance and Motor Unit Firing Behavior. *Journal of Neurophysiology*, 80(3):1373–1382, 1998. URL `http://jn.physiology.org/content/80/3/1373.abstract`.

[4] Ben Aisen. A Comparison of Multiclass SVM Methods. `http://courses.media.mit.edu/2006fall/mas622j/Projects/aisen-project/index.html`, December 2006.

[5] Leia B. Bagesteiro and Robert L. Sainburg. Handedness: Dominant Arm Advantages in Control of Limb Dynamics. *Journal of Neurophysiology*, 88(5):2408–2421, 2002. doi: 10.1152/jn.00901.2001. URL `http://jn.physiology.org/content/88/5/2408.abstract`.

[6] Mark F. Bear, Barry W. Connors, and Michael A. Paradiso. *Neuroscience: Exploring the Brain*. Lippincott Williams & Wilkins, 2006. ISBN 0781760038.

[7] C. M. Bishop. *Pattern Recognition and Machine Learning*. Springer, 2007.

[8] S. Bitzer and P. van der Smagt. Learning EMG control of a robotic hand: towards active prostheses. In *Robotics and Automation, 2006. ICRA 2006. Proceedings 2006 IEEE International Conference on*, pages 2819 –2823, may 2006. doi: 10.1109/ROBOT.2006.1642128.

[9] Paolo Bonato, Tommaso D'Alessio, and Marco Knaflitz. A Statistical Method for the Measurement of Muscle Activation Intervals from Surface Myoelectric Signal During Gait. *IEEE Transactions on Biomedical Engineering*, 45(3):287–299, March 1998.

[10] Reza Boostani and Mohammad Hassan Moradi. Evaluation of the forearm EMG signal features for the control of a prosthetic hand. *Physiological Measurement*, 24 (2):309, 2003. URL `http://stacks.iop.org/0967-3334/24/i=2/a=307`.

[11] Jürgen Bortz. *Statistik: für Sozialwissenschaftler (German Edition)*. Springer, 1999. ISBN 3540650881.

[12] J. Butterfass, M. Grebenstein, H. Liu, and G. Hirzinger. DLR-Hand II: next generation of a dextrous robot hand. In *Robotics and Automation, 2001. Proceedings 2001 ICRA. IEEE International Conference on*, volume 1, pages 109 – 114 vol.1, 2001. doi: 10.1109/ROBOT.2001.932538.

[13] Claudio Castellini and Patrick van der Smagt. Surface EMG in advanced hand prosthetics. *Biological Cybernetics*, 100:35–47, 2009. ISSN 0340-1200. URL `http://dx.doi.org/10.1007/s00422-008-0278-1`. 10.1007/s00422-008-0278-1.

[14] Chih-Chung Chang and Chih-Jen Lin. LIBSVM: A library for support vector machines. *ACM Transactions on Intelligent Systems and Technology*, 2(3):27:1 – 27:27, 2011.

[15] Scott Day. Important Factors in Surface EMG Measurement. Bortec Biomedical. `http://www.bortec.ca/pages/resources.htm` (accessed October 11, 2011).

[16] Carlo J. de Luca. The use of surface electromyography in biomechanics. *Journal of Applied Biomechanics*, 13(2):135 – 163, 1997.

[17] Carlo J. de Luca. Surface Electromygraphy: Detection and Recording. DelSys Incorporated, 2002.

[18] Louise Pyndt Diederichsen, Jesper Nørregaard, Poul Dyhre-Poulsen, Annika Winther, Goran Tufekovic, Thomas Bandholm, Lars Raundal Rasmussen, and Michael Krogsgaard. The effect of handedness on electromyographic activity of human shoulder muscles during movement. *Journal of Electromyography and Kinesiology*, 17(4):410 – 419, 2007. ISSN 1050-6411. doi: 10.1016/j.jelekin.2006.03.004. URL `http://www.sciencedirect.com/science/article/pii/S1050641106000393`.

[19] Richard Drake, Wayne Vogl, and Adam Mitchell. *Gray's Anatomy for Students*. Churchill Livingstone, 2004. ISBN 0443066124.

[20] K. Englehart and B. Hudgins. A robust, real-time control scheme for multifunction myoelectric control. *Biomedical Engineering, IEEE Transactions on*, 50(7):848 – 854, july 2003.

[21] Kevin Brian Englehart. *Signal Representation for Classification of the Transient Myoelectric Signal.* PhD thesis, The University of New Brunswick, October 1998.

[22] Dario Farina, LauraA.C. Kallenberg, Roberto Merletti, and HermieJ. Hermens. Effect of side dominance on myoelectric manifestations of muscle fatigue in the human upper trapezius muscle. *European Journal of Applied Physiology*, 90:480–488, 2003. ISSN 1439-6319. URL `http://dx.doi.org/10.1007/s00421-003-0905-4`. 10.1007/s00421-003-0905-4.

[23] FNIMH Henry Gray F.R.S. *Gray's Anatomy: The Unabridged Running Press Edition Of The American Classic.* Running Press, 1974. ISBN 0914294083.

[24] Björn Gerdle, Stefan Karlsson, Scott Day, and Mats Djupsjöbacka. *Acquisition, Processing and Analysis of the Surface Electromyogram.* Springer, 1999.

[25] L. J. Hargrove, K. Englehart, and B. Hudgins. A comparison of surface and intramuscular myoelectric signal classification. *IEEE Transactions on Biomedical Engineering*, 54(5):847–853, May 2007.

[26] Trevor Hastie, Robert Tibshirani, and Jerome Friedmann. *The Elements of Statistical Learning.* Springer Verlag, 2 edition, 2009. ISBN 978-0-387-84857-0.

[27] P. Horki, T. Solis-Escalante, C. Neuper, and G. Müller-Putz. Combined motor imagery and SSVEP based BCI control of a 2 DoF artificial upper limb. *Medical and Biological Engineering and Computing*, 2011. doi: 10.1007/s11517-011-0750-2.

[28] Chih-Wei Hsu and Chih-Jen Lin. A comparison of methods for multiclass support vector machines. *Neural Networks, IEEE Transactions on*, 13(2):415 –425, March 2002. ISSN 1045-9227. doi: 10.1109/72.991427.

[29] Jeremy Hsu. The Future of Video Game Input: Muscle Sensor. `http://www.livescience.com/5836-future-video-game-input-muscle-sensors.html`, October 2009.

[30] B. Hudgins, P. Parker, and R.N. Scott. A new strategy for multifunction myoelectric control. *Biomedical Engineering, IEEE Transactions on*, 40(1):82 –94, jan. 1993. ISSN 0018-9294. doi: 10.1109/10.204774.

[31] Zhonglin Lin, Changshui Zhang, Wei Wu, and Xiaorong Gao. Frequency Recognition Based on Canonical Correlation Analysis for SSVEP-Based BCIs. *Biomedical Engineering, IEEE Transactions on*, 54(6):1172 –1176, june 2007. ISSN 0018-9294.

[32] Herbert Lippert. *Anatomie Text und Atlas*. Urban u. Schwarzenberg, 6 edition, 1995. ISBN 3-541-07216-4.

[33] Yi-Hung Liu, Han-Pang Huang, and Chang-Hsin Weng. Recognition of Electromyographic Signals Using Cascaded Kernel Learning Machine. *Mechatronics, IEEE/ASME Transactions on*, 12(3):253 –264, june 2007. ISSN 1083-4435. doi: 10.1109/TMECH.2007.897253.

[34] Marie-Françoise Lucas, Adrien Gaufriau, Sylvain Pascual, Christian Doncarli, and Dario Farina. Multi-channel surface EMG classification using support vector machines and signal-based wavelet optimization. *Biomedical Signal Processing and Control*, 3(2):169 – 174, 2008. ISSN 1746-8094. doi: 10.1016/j.bspc.2007.09.002. URL `http://www.sciencedirect.com/science/article/pii/S1746809407000791`. <ce:title>Surface Electromyography</ce:title> <ce:subtitle>Surface Electromyography</ce:subtitle>.

[35] Roberto Merletti. Standards for Reporting EMG Data. *Journal of Electromyography and Kinesiology*, 9:III–IV, 1999.

[36] G. Müller-Putz and C. Neuper. Trends in der Neurorehabilitation. Lecture notes, Graz University of Technology, 2011.

[37] T.G. Oesterlein. Monocular steady-state visual evoked potential based brain-computer interfaces by utilizing frequency/phase relationships. Master's thesis, Graz University of Technology, 2012.

[38] M.A. Oskoei and Huosheng Hu. Support Vector Machine-Based Classification Scheme for Myoelectric Control Applied to Upper Limb. *Biomedical Engineering, IEEE Transactions on*, 55(8):1956 –1965, aug. 2008. ISSN 0018-9294. doi: 10.1109/TBME.2008.919734.

[39] C. Perez-Maldonado, A.S. Wexler, and S.S. Joshi. Two-Dimensional Cursor-to-Target Control From Single Muscle Site sEMG Signals. *Neural Systems and Rehabilitation Engineering, IEEE Transactions on*, 18(2):203 –209, april 2010. ISSN 1534-4320. doi: 10.1109/TNSRE.2009.2039394.

[40] G. Pfurtscheller, B. Z. Allison, C. Brunner, G. Bauernfeind, T. Solis-Escalante, R. Scherer, T. O. Zander, G. Müller-Putz, C. Neuper, and N. Birbaumer. The hybrid BCI. *Frontiers in Neuroscience*, 4:30, 2010. doi: 10.3389/fnpro.2010.00003.

[41] Angkoon Phinyomark, Chusak Limsakul, and Pornchai Phukpattaranont. A Novel Feature Extraction for Robust EMG Pattern Recognition. *Journal of Computing*, 1:71 – 80, 2009.

[42] Danny Plass-Oude Bos, Boris Reuderink, Bram Laar, Hayrettin Gürkök, Christian Mühl, Mannes Poel, Anton Nijholt, and Dirk Heylen. Brain-Computer Interfacing and Games. In Desney S. Tan and Anton Nijholt, editors, *Brain-Computer Interfaces*, Human Computer Interaction Series, pages 149–178. Springer London, 2010. ISBN 978-1-84996-272-8.

[43] Markus Pröll. Using a Low-Cost Gyro and EEG-based Input Device in Interactive Game Design. Master's thesis, Graz University of Technology, 2012.

[44] J. Rafiee, M.A. Rafiee, F. Yavari, and M.P. Schoen. Feature extraction of forearm EMG signals for prosthetics. *Expert Systems with Applications*, 38(4):4058 – 4067, 2011. ISSN 0957-4174. doi: 10.1016/j.eswa.2010.09.068. URL http://www.sciencedirect.com/science/article/pii/S0957417410010250.

[45] N.S. Rekhi, A.S. Arora, S. Singh, and D. Singh. Multi-Class SVM Classification of Surface EMG Signal for Upper Limb Function. In *Bioinformatics and Biomedical Engineering , 2009. ICBBE 2009. 3rd International Conference on*, pages 1 –4, june 2009. doi: 10.1109/ICBBE.2009.5163093.

[46] Robert L. Sainburg and Sydney Y. Schaefer. Interlimb Differences in Control of Movement Extent. *Journal of Neurophysiology*, 92(3):1374–1383, 2004. doi: 10.1152/jn.00181.2004. URL http://jn.physiology.org/content/92/3/1374.abstract.

[47] R. Scherer, G. R. Müller-Putz, and G. Pfurtscheller. Flexibility and practicality: Graz brain-computer interface approach. *International Review of Neurobiology*, 86: 119–131, 2009. doi: 10.1016/S0074-7742(09)86009-1.

[48] A. Schlogl and C. Brunner. BioSig: A Free and Open Source Software Library for BCI Research. *Computer*, 41(10):44 –50, oct. 2008. ISSN 0018-9162. doi: 10.1109/MC.2008.407.

[49] Alois Schlögl. GDF - A general dataformat for BIOSIGNALS. *CoRR*, abs/cs/0608052, 2006.

[50] Xing Shusong and Zhang Xia. EMG-driven computer game for post-stroke rehabilitation. In *Robotics Automation and Mechatronics (RAM), 2010 IEEE Conference on*, pages 32 –36, june 2010. doi: 10.1109/RAMECH.2010.5513218.

[51] Gerhard Staude, Claus Flachenecker, Martin Daumer, and Werner Wolf. Onset Detection in Surface Electromyographic Signals: A Systematic Comparison of Methods. *EURASIP Journal on Applied Signal Processing*, 2:67–81, 2001.

[52] F. Tenore, A. Ramos, A. Fahmy, S. Acharya, R. Etienne-Cummings, and N.V. Thakor. Towards the Control of Individual Fingers of a Prosthetic Hand Using Surface EMG Signals. In *Engineering in Medicine and Biology Society, 2007. EMBS 2007. 29th Annual International Conference of the IEEE*, pages 6145 –6148, aug. 2007. doi: 10.1109/IEMBS.2007.4353752.

[53] F.V.G. Tenore, A. Ramos, A. Fahmy, S. Acharya, R. Etienne-Cummings, and N.V. Thakor. Decoding of Individuated Finger Movements Using Surface Electromyography. *Biomedical Engineering, IEEE Transactions on*, 56(5):1427 –1434, may 2009. ISSN 0018-9294. doi: 10.1109/TBME.2008.2005485.

[54] Dennis Tkach, He Huang, and Todd A Kuiken. Study of stability of time-domain features for electromyographic pattern recognition. *Journal of Neuroengineering and Rehabilitation*, 7(21):13, 2010.

[55] Vladimir N. Vapnik. *The Nature of Statistical Learning Theory*. Springer Verlag, 1995. ISBN 0-387-94559-8.

[56] François-Benoît Vialatte, Monique Maurice, Justin Dauwels, and Andrzej Cichocki. Steady-state visually evoked potentials: Focus on essential paradigms and future perspectives. *Progress in Neurobiology*, 90(4):418 – 438, 2010. ISSN 0301-0082. doi: 10.1016/j.pneurobio.2009.11.005. URL http://www.sciencedirect.com/science/article/pii/S0301008209001853.

[57] K.R. Wheeler and C.C. Jorgensen. Gestures as input: neuroelectric joysticks and keyboards. *Pervasive Computing, IEEE*, 2(2):56 – 61, april-june 2003. ISSN 1536-1268. doi: 10.1109/MPRV.2003.1203754.

[58] J. R. Wolpaw, N. Birbaumer, D. J. McFarland, G. Pfurtscheller, and T. M. Vaughan. Brain-computer interfaces for communication and control. *Clinical Neurophysiology*, 113:767–791, 2002. doi: 10.1016/S1388-2457(02)00057-3.

[59] M. Yoshikawa, M. Mikawa, and K. Tanaka. Hand Pose Estimation Using EMG Signals. In *Engineering in Medicine and Biology Society, 2007. EMBS 2007. 29th Annual International Conference of the IEEE*, pages 4830 –4833, aug. 2007. doi: 10.1109/IEMBS.2007.4353421.

[60] M. Zardoshti-Kermani, B.C. Wheeler, K. Badie, and R.M. Hashemi. EMG feature evaluation for movement control of upper extremity prostheses. *IEEE Transactions onRehabilitation Engineering*, 3(4):324 –333, dec 1995. doi: 10.1109/86.481972.

[61] M. Zecca, S. Micera, M. Carrozza, and P. Dario. Control of multifunctional prosthetic hands by processing the electromyographic signal. *Critical Reviews in Biomedical Engineering*, 30(4–6):459–485, 2002.